UC San Diego

UC San Diego Electronic Theses and Dissertations

Title

Molecular and activity-dependent mechanisms of synaptic refinement

Permalink

https://escholarship.org/uc/item/0xj3x9d1

Author

Sylwestrak, Emily Lauren

Publication Date

2011

Peer reviewed|Thesis/dissertation

eScholarship.org Powered by the California Digital Library
University of California

UNIVERSITY OF CALIFORNIA, SAN DIEGO

Molecular and Activity-Dependent Mechanisms of Synaptic Refinement

A dissertation submitted in partial satisfaction of the requirements for the degree

Doctor of Philosophy

in

Neurosciences

by

Emily Lauren Sylwestrak

Committee in charge:

Professor Darwin Berg, Chair
Professor Anirvan Ghosh
Professor Teru Nakagawa
Professor Samuel Pfaff
Professor Massimo Scanziani

2011

The dissertation of Emily Lauren Sylwestrak is approved, and it is acceptable in quality and form for publication on microfilm and electronically:

Chair

University of California, San Diego

2011

DEDICATION

To John and Mary Lou Sylwestrak

TABLE OF CONTENTS

LIST OF ABBREVIATIONS

1. ISH: In situ hybridization
2. AMPA: 2-amino-3-(5-methyl-3-oxo-1,2- oxazol-4-yl) propanoic acid
3. NMDA: *N-Methyl-D-aspartate*
4. OLM: Oriens/lacunosum moleculare
5. EPSC: Excitatory postsynaptic current
6. LRR: Leucine-rich repeat
7. CNS: Central Nervous system
8. GFP: Green fluorescent protein
9. DIV: Day *in vitro*
10. PSD: Postsynaptic Density
11. GAPDH: Glyceraldehyde 3-phosphate dehydrogenase
12. VGLUT: vesicular glutamate transporter
13. GAD: glutamic acid decarboxylase
14. CamKII: Ca^{2+}/Calmodulin-Dependent protein kinase II
15. SST: Somatostatin
16. PV: Parvalbumin
17. Calb: Calbindin
18. KO: Knockout
19. WT: Wild-type
20. Elfn: Extracellular Leucine-rich repeat fibronectin containing
21. MeCP2: Methyl-CpG binding protein 2
22. shRNA; short hairpin RNA
23. TTX: Tetrodotoxin

24. DNQX: 6,7-dinitroquinoxaline-2,3-dione
25. APV: (2R)-amino-5-phosphonovaleric acid
26. Bic: Bicuculline
27. LRRTM2: Leucine-rich repeat transmembrane 2
28. FNIII: Fibronectin Type-III
29. Ig: Immoglobulin
30. s.r.: Stratum radiatum
31. s.p.: Stratum pyramidale
32. s.o.: Stratum oriens
33. MK801: (+)-5-methyl-10,11- dihydro-5*H*-dibenzo[*a*,*d*]cyclohepten-5,10-imine maleat, Dizocilpine

LIST OF FIGURES

ACKNOWLEDGEMENTS

I would like to thank Professor Anirvan Ghosh for this unwavering support as my thesis advisor. His guidance has been formative in the production of this thesis and his mentorship has influenced the way I think and work as a scientist.

I would like to thank all of the members of the Ghosh Lab for their advice and friendship during my graduate career. With encouragement and laughter, they make it possible to work long hours on projects fraught by difficulty. I would especially like to thank my fellow graduate students, Beth Ripley, Beth Davis, Scott Wilke, Matthew O'Sullivan, and Laura DeNardo, whose camaraderie I have appreciated. Matthew and Laura have also provided frequent experimental advice, which has greatly helped in producing the work presented here.

Postdoctoral fellows have also supported this work. In particular I would like to thank Joris deWitt and Zilong Qiu. Joris deWitt has provided invaluable guidance and support on the work presented in Chapters 2 and 3. His patience and willingness to help is greatly appreciated. Zilong Qui proposed the initial project and motivation behind the work presented in Chapter 5 and has been integral to its completion. The resulting manuscript titled "The Rett Syndrome Protein MeCP2 Regulates Synaptic Scaling" is in press, on which we are co-authors with David N. Lieberman, Yan Zhang, Xin-Yu Liu, Anirvan Ghosh as additional contributing authors.

VITA

2006	Bachelor of Science, University of Illinois, Urbana-Champaign
2006-2011	Research Assistant, University of California, San Diego
2010	Master of Science, University of California, San Diego
2011	Doctor of Philosophy, University of California, San Diego

PUBLICATIONS

de Wit J, Sylwestrak E, O'Sullivan ML, Otto S, Tiglio K, Savas JN, Yates JR 3rd, Comoletti D, Taylor P and Ghosh A (2009) LRRTM2 Interacts with Neurexin1 and Regulates Excitatory Synapse Formation. Neuron 64(6):799-806.

Li L, Bender KJ, Drew PJ, Jadhav SP, Sylwestrak E, Feldman DE (2009) Endocannabinoid signaling is required for development and critical period plasticity of the whisker map in somatosensory cortex. Neuron 64(4):537-549.

Beatty JA, Sylwestrak EL, Cox CL (2009) Two distinct populations of projection neurons in the rat lateral parafascicular thalamic nucleus and their cholinergic responsiveness. Neuroscience 162:155-173.

ABSTRACT OF THE DISSERTATION

Molecular and Activity-Dependent Mechanisms of Synaptic Refinement

By

Emily Lauren Sylwestrak

Doctor of Philosophy in Neurosciences

University of California, San Diego, 2011

Professor Darwin Berg, Chair

In order to execute complex behavioral tasks, neural circuits must be precisely connected and each connection must be finely tuned. Neural circuits are shaped by molecular mechanisms that regulate the establishment of synaptic connections, as well as by changes in activity, which modifies those circuits. Both processes are needed to support a functional, plastic neural circuit.

In the hippocampus, CA1 axons make divergent connections onto several classes of local interneurons. Remarkably, the presynaptic properties of each synapse depend on the identity of the post-synaptic partner. Synapses from CA1 axons onto basket cells exhibit short-term depression, whereas those onto oriens-lacunosum molecular (OLM) interneurons are strongly facilitating (Ali et al., 1998; Ali

and Thomson, 1998). The molecular mechanisms underlying such target-cell specific synaptic specification remain unknown.

Here we show that Elfn1, a single-pass transmembrane protein with extracellular leucine-rich repeat (LLR) and fibronectin type 3 (FN3) domains, is expressed selectively by OLM interneurons and localizes to excitatory synapses. Lentiviral-mediated postsynaptic knockdown of Elfn1 in OLM interneurons strongly reduces short-term facilitation and increases the amplitude of synaptic currents. These effects are explained by an increase in presynaptic release probability, while postsynaptic properties are left unaffected. Thus, Elfn1 regulates facilitation at the CA1-OLM synapse by acting trans-synaptically to reduce presynaptic probability of release. These observations indicate that cell- and synapse- specific expression of LRR- containing proteins in postsynaptic neurons can contribute to the generation of functional synaptic diversity.

Activity-dependent modification, in addition to molecular mechanisms, can shape synaptic function. Synaptic scaling is a form of homeostatic synaptic plasticity characterized by cell-wide changes in synaptic strength in response to changes in overall levels of neuronal activity. Here we report that bicuculline-induced increase in neuronal activity leads to a decrease in mEPSC amplitude and a decrease in expression of the AMPA receptor subunit GluR2 in rat hippocampal cultures. Bicuculline treatment also leads to an increase in the levels of the transcriptional repressor MeCP2, which binds to the GluR2 promoter along with the co-repressors HDAC1 and mSin3A. Down-regulation of MeCP2 by shRNA expression or genetic deletion blocks the bicuculline-induced decrease in GluR2 expression and mEPSC amplitude. These observations indicate that MeCP2 mediates activity-dependent synaptic scaling, and suggest that the pathophysiology of Rett syndrome, which is caused by mutations in MeCP2, may involve defects in activity-dependent regulation

of synaptic currents. Taken together, these studies on the role of Elfn1 in target-cell specificity and MeCP2 regulation of synaptic scaling present novel roles for molecules in the specification and activity-dependent regulation of synapses.

CHAPTER 1: INTRODUCTION

1.1 NEURONAL CIRCUITS ARE PRECISELY CONNECTED AND ACTIVITY-REGULATED

The mammalian brain contains distinct circuits that process different streams of sensory input to produce different behavioral outputs. For example, the visual cortex, cerebellum, and hippocampus each comprise specialized circuits that process vision, movement, and memory, respectively. Precise connectivity between heterogeneous populations of neurons defines the framework of the circuit, within which neurons are connected by specialized synapses whose physiological properties depend on pre- and postsynaptic cell types. The resulting circuit is defined both by its component cells and by the properties of their synaptic connections to each other. Moreover, synaptic function can be modified by recent activity, in some cases by mechanisms engaged on the timescale of milliseconds and others, over many hours. Although much is known about the diversity of synaptic properties, the molecular mechanisms that regulate synaptic transmission in a cell-type specific manner or in different activity regimes remain unknown, though they are fundamental to the function of the nervous system. This study describes my efforts to determine the role of synaptic organizing proteins in regulating synapse-specific properties as well as the role of transcriptional regulation in activity-dependent modulation of synaptic function. Much work has contributed to our understanding of synaptic function and has informed the experiments described in this dissertation. An overview of the relevant advances will be presented in Chapter 1. The first part of Chapter 1 will examine what is known about normal synaptic function, in particular, how axons demonstrate target cell-specific function and how synaptic proteins localize to specific synapses. In the second half, I will address previous studies showing how synapses can be modified by activity and what molecular mechanisms are responsible for activity-induced changes.

1.2 CIRCUIT FORM AND FUNCTION

A typical microcircuit contains principal neurons, interneurons, afferent input, efferent output and local connections. Hippocampal circuits display these ubiquitous features and are useful models for studying the general principles of circuit formation and function. In subregions of the hippocampus, microcircuits can readily be identified and analyzed. As CA1 is a focus of this study, it will be useful to understand the general organization of the CA1 connectivity (Figure 1.1). In brief, the circuit consists of convergent excitatory input, local inhibitory connections, and divergent excitatory output. Afferents arrive from the entorhinal cortex via the temporoammonic pathway and from the CA3 region via the Schaffer collaterals, creating two spatially segregated synaptic inputs. Schaffer collateral axons synapse on two different cell types, CA1 pyramidal cells and parvalbumin (PV) positive interneurons. The PV interneurons, also called basket cells, form specialized axonal arbors that encapsulate CA1 pyramidal cell somata with inhibitory synapses. They provide feed forward inhibition. Strong inhibitory input from PV cells, slowed by a disynaptic delay, curtails direct excitatory input from Schaffer collaterals, thereby limiting CA1 pyramidal cell spiking to a precise temporal window (Pouille and Scanziani, 2001).

CA1 pyramidal cell output is also divergent. CA1 axons project to the subiculum and entorhinal cortex, but they also make local connections with CA1 interneurons. Local synapses primarily contact PV basket cells and another interneuron population, oriens lacunosum moleculare (OLM) interneurons. Both, in turn, synapse back on CA1 pyramidal cells, providing feedback inhibition. PV cells inhibit pyramidal cell somata whereas OLM cells inhibit pyramidal cell distal apical dendrites. The properties of CA1

synapses onto PV and OLM interneurons are quite different. Pyramidal cell-PV synapses, like most other synapses onto interneurons, show short-term depression, as each subsequent action potential in a stimulus train yields a smaller postsynaptic response. In contrast, CA1 synapses onto OLM cells are unique among interneurons; they are strongly facilitating (Lacaille et al., 1987; Ali and Thomson, 1998).

Ultimately, the short-term facilitation or depression of CA1-PV and CA1-OLM synapses, respectively, underpin their roles in the circuit. Namely, the strong, but quickly depressing synapse onto PV cells encodes the onset of activity in CA1. Facilitating synapses onto OLM cells recruit these cells only after repeated pyramidal cell spiking, making them sensitive to the rate of activity in CA1 (Pouille and Scanziani, 2004). Furthermore, it is crucial to note that the hallmark difference between these two synapses from the same axon, namely short-term facilitation or depression, is of presynaptic origin (Wu and Saggau, 1994; Zucker and Regehr, 2002). Therefore, axons can identify postsynaptic cell type and regulate presynaptic properties according to the postsynaptic partner, a phenomenon called target-cell specificity. Although it is essential for the routing of inhibition in the hippocampus, the mechanism by which CA1 axons tailor properties according to target-cell type is unknown.

1.3 Information transfer depends on the properties of individual synapses

Regulation of synaptic transmission

CA1 axons clearly demonstrate that circuit function relies on the properties of synaptic transmission at different synaptic connections. At each step in synaptic transmission, the function of specific components can be modified. At the most basic level, synaptic transmission occurs when an action potential invades the presynaptic

terminal, opening voltage-sensitive calcium channels. Increases in intracellular calcium trigger the fusion of docked vesicles with the plasma membrane, releasing glutamate into the synaptic cleft. Glutamate binds to postsynaptic receptors, such as AMPA or NMDA receptors, depolarizing the postsynaptic membrane. Many important advances have been made in our understanding of how modulating each of these steps, on both the presynaptic and postsynaptic side, can alter synaptic transmission.

Presynaptic changes in synaptic transmission affect the probability, time course, or magnitude of vesicular release, determining the glutamate concentration seen by the postsynaptic cell. Calcium channels provide the first locus of synaptic regulation. Since calcium increases trigger vesicle fusion, the dynamics of calcium transients is tightly coupled to glutamate release. The number of calcium channels affects the absolute magnitude of presynaptic calcium transients. In addition, there are several different types of calcium channels that vary in single channel conductance and kinetics, further changing the size and temporal dynamics of the calcium transient (Fisher and Bourque, 2001). Upon channel opening, calcium diffuses from the channel to the release machinery; therefore, the distance from channels to docked vesicles and the presence of endogenous calcium buffers shape the spatiotemporal dynamics of calcium transients (Atwood and Karunanithi, 2002). The number of docked vesicles available for release and the rate at which they are replenished also vary from synapse to synapse and can likewise influence release.

Ultimately, changing each of these presynaptic parameters can produce terminals with the full spectrum of release properties, from synapses that require many action potentials to release neurotransmitter, to those that will reliably release it on every action potential. Differential release properties underlie the short-term facilitation and short-term depression mentioned above in the CA1 circuit. Initial probability of release is

lower CA1-OLM synapses than CA1-PV synapses (Biro et al., 2005; Sun et al., 2005). Thus, more vesicles will be released at PV synapses on the first stimulus in a train. During repetitive stimulation of the CA1 axons; however, calcium cannot be fully cleared from the presynaptic terminal. When subsequent stimuli arrive, the residual calcium will sum with the next calcium transient. This affects the two synapses differently. For the OLM synapse, increased calcium concentration triggers more vesicles to be released. For the PV synapse, the first stimulus depleted many of its readily-releasable vesicles, so despite an increase in calcium, the response will be smaller since fewer vesicles are available for release. CA1 axons demonstrate how neurons can tightly regulate presynaptic properties to generate synapses that are either facilitating or depressing.

On the postsynaptic side, receptors, typically ionotropic AMPA- or NMDA-sensitive receptors, detect glutamate release by the presynaptic terminal and open to depolarize the postsynaptic cell. Changes in the number or type of glutamate receptors affect the size and time course of postsynaptic depolarization. For example, during certain patterns of activity, the postsynaptic response to presynaptic vesicular release can be strengthened, a process called long-term potentiation (LTP). LTP results from the insertion of AMPA receptors to the postsynaptic membrane, increasing the size of the postsynaptic depolarization. The types of glutatmate receptors present can also be regulated. For instance, the presence of GluR2-lacking AMPARs changes AMPAR conductance and calcium permeability (Koh et al., 1995). Similarly, NMDAR conductance and desensitization depends on which subunit it contains (NR2A-D) (Krupp et al., 1996; Momiyama et al., 1996; Vicini et al., 1998).

Adjusting each of these synaptic variables can produce a diversity of functional synaptic phenotypes. Yet, synapses are not merely a stochastic combination of these parameters. Many have a predictable constellation of properties that depends on the

identity of the pre- and postsynaptic cell types. While there has been extensive characterization of the properties of hippocampal synapses, the mechanisms that tailor presynaptic properties to postsynaptic cell type, as in the CA1 pyramidal cell to interneuron synapse, are unclear.

Synaptic Organizing Complexes

One intriguing possibility is that accessory synaptic proteins may organize synaptic components in different ways depending on the pre- and postsynaptic partners. Synaptic complexes include transsynaptic adhesion molecules, ion channels and cytosolic proteins. Many studies have demonstrated that cytosolic scaffolding proteins act as a hub, anchoring synaptic proteins. Of these, PSD-95 has been most extensively studied and shows binding domains that can interact with many types of postsynaptic components: Tarps, NMDARs, and kainate receptors (Kim and Sheng, 2004; Han and Kim, 2008). In addition to structuring the cytosolic components, transmembrane or membrane associated proteins also organize extracellular interactions (Mcmahon and Díaz, 2011). Neuronal cell adhesion molecule (NCAM) was the first such molecule identified (Rutishauser et al., 1988). This and other similarly functioning transmembrane proteins have been called cell-adhesion molecules. However, more recent work has shown that many cell-adhesion molecules are more than synaptic glue. In fact, several studies have begun to show how cell adhesion molecules can instruct synapse formation and recruit core synaptic components (Shen and Scheiffele, 2010).

Cell adhesion molecules are a diverse group of proteins unified by the role they play in extracelluar interactions on the pre- and postsynaptic surfaces. The instructive nature of their interactions was first demonstrated in culture, where it was shown that heterologous cells expressing the synaptic transmembrane protein neuroligin (Song et

al., 1999) induce the formation of hemisynapses on contacting axons (Scheiffele et al., 2000). It was subsequently shown that this phenomenon was the result of an interaction with the presynaptic transmembrane partner neurexin (Scheiffele, 2003). The robust phenotype of neurexin-neuroligin binding suggested it was a key player in nascent synapse formation. However, knockout of each of the neuroligin genes produced a subtle phenotype, with the primary deficits arising in synapse function, rather than formation (Varoqueaux et al., 2006). This suggests that there may be a variety of neurexin-neuroligin like proteins that exhibit functional redundancy. It is possible that each one has slightly different interactions and through their combinatorial expression synapses acquire specific properties.

In support of the potential their role in generating synaptic diversity, many cell adhesion molecules are extensively spliced, leading to the possibility that a relatively small set of genes can create a variety of different synaptic interactions. For example, the protocadherin protein family is considerably spliced, and single cell RTPCR has shown that protocadherin isoforms are differentially expressed between neighboring cells (Esumi et al., 2005; Morishita and Yagi, 2007). Similarly, down-syndrome cell adhesion molecules (DSCAMs) are extensively spliced and multiple isoforms are stochastically expressed in drosophila neurons (Hattori et al., 2007). Homophilic DSCAM interactions are repulsive and neighboring dendrites from a single neuron express the same complement of isoforms, providing a system for self avoidance (Matthews et al., 2007). Neurexins are also alternatively spliced, with enough splice variants to possibly produce hundreds of isoforms, although it is unclear how these are distributed among neurons in the brain (Ullrich et al., 1995). Neurexins are particularly promising, as it has been shown that neurexin receptors can bind in an isoform-dependent manner. Neurexins have splice site-specific binding to postsynaptic proteins

such as Cerebellin-GluRδ2 and LRRTM2 (Fisher and Bourque, 2001; de Wit et al., 2009b; Uemura et al., 2010). While many cell adhesion proteins have been shown to regulate aspects of synapse formation and exhibit great structural diversity, in the past, most studies have used culture systems with unidentified synapses, operating under the assumption that synaptic properties are homogenous. More recently, however, some studies have focused on the function of cell-type specific synaptic proteins.

Synapse-specific molecules

The variety of genes and isoforms of synaptic transmembrane proteins has fueled interest in the role of transsynaptic signaling molecules in the establishment of specific sets of synapses. To date, most molecules identified have been relatively ubiquitously expressed at broad classes of synapses. For example, different neuroligins have been shown to be present at excitatory (neuroligin 1) or inhibitory synapses (neuroligin 2). Other synaptic adhesion molecules, such as N-CAM, N-Cad, or SALMs are also broadly expressed. More recently, attention has focused on synaptic molecules with more restricted expression. In the hippocampus, CA1 pyramidal cells receive laminarly-segregated input from CA3 and entorhinal cortex in the stratum radiatum and stratum lacunosum moleculare, respectively. These two axonal populations express different Netrin-Gs (Netrin G1 and Netrin G2), which are GPI anchored extracellular proteins that bind to specific postsynaptic Netrin-G ligands (NGL1 and NGL2) (Figure 1.2). Knocking out the presynaptic Netrin-Gs abolishes the laminar segregation of postsynaptic NGLs, suggesting these interactions are important for creating regulating Schaffer collateral and temporoammonic pathways (Nishimura-Akiyoshi et al., 2007). In CA3, mossy fiber synapses on CA3 pyramidal cells are very specialized hippocampal synapses, both structurally and functionally. Mossy fiber axons produce large boutons

that engulf specialized CA3 postsynaptic structures called thorny excrescences, which have densely packed multi-headed spines. This is a particularly potent synapse and shows strong paired-pulse facilitation. Cadherin-9 is present on pre- and postsynaptic membranes and has been shown regulate number and size of mossy fiber synapses onto CA3 cells *in vitro* and regulate the morphology of the synapse *in vivo*. Cadherin-9 knockdown drastically increases the number of immature-like filopodia on CA3 dendrites and reduces the number of mossy fiber boutons (Williams et al. 2011). It will be interesting to determine if manipulating Cadherin-9 has any consequence for synaptic function at mossy fiber synapses. Like the hippocampus, the cerebellum is a highly ordered structure that facilitates synapse-type identification. At the parallel fiber synapse onto Purkinje cells, GluRδ2 forms a synaptic complex with cerebellin1 and neurexin. This interaction is dependent on the alternative splicing at neurexin splice site 4 (Uemura et al.). At another site on the Purkinje cell, basket cells make unique connections, called pinceau synapses, onto the axon initial segment. It has been shown that the cell adhesion molecule neurofascin is found in Purkinje cells and localizes specifically to the axon initial segment. Presence of this target-derived factor restricts basket cells axons to the axon initial segment (Ango et al., 2004). Each of these receptor-ligand pairs provides evidence for the notion that, in addition to the core synaptic components, the nervous system has a heterogeneously distributed set of accessory synaptic proteins that may serve to alter synaptic localization, structure, or function.

Transynaptic molecules are candidates for target-cell specificity

Although the examples listed above show that synaptic organizing molecules can be localized to specific synapses or are necessary for their formation, there is little evidence that these molecules can regulate functional properties unique to those

synapses. The target-cell specificity that arises at CA1 synapses onto interneurons requires that the presynaptic terminals change their release properties depending on postsynaptic interneuron cell type. One possible solution to this problem is the presence of a target-derived cue that can signal retrogradely to the presynaptic terminal. We know that synaptic adhesion molecules can interact in *trans* with their synaptic partners and in *cis* to regulate pre- or postsynaptic machinery, making them ideal candidates to fulfill such a role. I propose that oriens interneurons differentially express specific cell adhesion molecules that cue CA1 axons to regulate presynaptic release, producing different short-term plasticity at the two synapses. In Chapters 2-4, I show that the novel postsynaptic transmembrane protein, Elfn1, regulates target-cell specific short-term facilitation at CA1 synapses.

1.4 SYNATPIC FUNCTION IS ADAPTIVE

Activity shapes neuronal connectivity

Synaptic properties are not static, but dynamic. Although synaptic organizing molecules can regulate synaptic elements to establish a functional set point for the synapse, the recent history of the synapse can push it away from that set point. Furthermore, activity can affect synapses on many different timescales and organizational levels. The timescale for activity-dependent changes can range from milliseconds to hours. For example, even in the short-term plasticity at CA1-OLM synapses, the recent history of the synapse (whether or not it received a stimulus in the past 50 ms) will affect the postsynaptic response. However, more often we think of activity-dependent changes occurring at longer timescales, from minutes to hours, and producing different effects on synaptic function depending on the pattern and duration of

activity. Activity also sculpts the nervous system on different structural levels. On the level of a sensory system, activity is necessary to organize developing circuits. In the visual system, alternating columns of cortex show preferential input from one eye, so intraocular injections will label stripes in the cortex corresponding to that eye's downstream targets, called ocular dominance columns. When sensory input from one eye is abolished during development by monocular deprivation, the ordered arrangement of ocular dominance columns disappears, demonstrating that the refinement of these circuits is activity-dependent (Hubel et al., 1977). On the level of individual connections, activity is also necessary for synaptic pruning. At the neuromuscular junction, supernumerary connections between motor neurons and muscle fibers are pruned during development, a process that is abolished in the absence of activity (Thompson, 1985). Furthermore, at individual synapses in the central nervous system, changes in synaptic activity result in strengthening or weakening, a process called synaptic plasticity. A fundamental question in neuroscience is how a neuron transforms changes in activity into changes in synaptic composition, at the level of individual synapses (Hebbian plasticity) and the cell as a whole (homeostatic plasticity).

Hebbian Plastity

Much work has been devoted to understanding how activity shapes synaptic function. Through this work, activity-dependent changes as described above have been broadly divided into two categories: Hebbian and non-hebbian plasticity. In Hebbian plasticity, the efficacy of a synaptic connection increases when a postsynaptic cell consistently fires with the presynaptic cell, but diminishes when it does not. This change is synapse specific, so individual connections between neurons can be modulated according to their recent activity. Bliss and Lomo first demonstrated this by examining

the change in the field EPSP after stimulating an afferent pathway in the hippocampus, which resulted in an increase in the field EPSP amplitude, whereas a control pathway that did not receive stimulation showed no change. The phenomenon persisted for hours following stimulation and was called long-term potentiation (LTP) (Bliss and Lomo, 1973). In the decades since their landmark experiment, many studies have explored the molecular mechanisms underpinning LTP and its counterpart, long-term depression (LTD). While the mechanisms of LTP vary with synapse type and are dependent upon the induction protocol, there are a few critical steps that apply to most forms of LTP. When a presynaptic input is strongly stimulated, often in conjunction with postsynaptic depolarization, calcium enters the post-synaptic compartment through calcium-permeable NDMA receptors. Increases in intracellular calcium activate CaMKII, which in turn promotes the insertion of AMPARs into the postsynaptic membrane. More AMPARs at the surface increase the conductance and result in a larger postsynaptic response. In contrast, intermittent use of a synapse results in moderate increases in postsynaptic calcium, either by activation of NMDARs or mGluRs. Small, slow increases in calcium result in the activation of phosphotases that promote AMPAR internalization (Collingridge et al., 2010). Thus, synapses can employ LTP and LTD to adjust synaptic strength depending on their levels of activity.

Homeostatic Plasticity

Without a counteracting mechanism, the forces of Hebbian plasticity would result in the polarization of synaptic strength, were synapses are either maximally strengthened, or completely eliminated. To balance this force it was proposed that a second, non-Hebbian type of plasticity might occur, broadly called homeostatic plasticity. Turrgiano and colleagues first demonstrated this by silencing neuronal cultures and

measuring quantal size by recording mEPSCs (Turrigiano et al., 1998). They found that chronic activity blockade results in an increase in the strength of all synapses onto a neuron. Moreover, each synaptic strength is increased in proportion to its original strength. This multiplicative scaling of synaptic strengths meant that a neuron could globally adjust absolute synaptic strength, but keep the relative strengths between synapses constant. In like vein, a chronic increase in synaptic activity produces a scaling down of synaptic strengths. These two opposing mechanisms may represent a way to keep firing rates within a range suitable for information processing while still maintaining the ability of Hebbian plasticity to influence the relative synaptic strengths.

In the past decade, synaptic scaling has been shown to include both pre- and postsynaptic changes, although the latter have been more prominent. At the presynaptic terminal, chronic activity blockade has been shown to change presynaptic release probability and the number of readily releasable synaptic vesicles (Bacci et al., 2001; Murthy et al., 2001). Conversely, increases in activity have been shown to reduce the readily releasable pool size (Moulder et al., 2006). Much more evidence exists for postsynaptic homeostatic changes in synaptic strength. Soon after the identification of synaptic scaling, O'Brien and colleagues reported an activity-dependent accumulation of AMPARs (O'Brien et al., 1998). Since then, many studies have focused on identifying the exact postsynaptic mechanisms responsible for homeostatic plasticity. In part, an increase in synaptic AMPARs arises from a newly synthesized receptor population (Ju et al., 2004). However, there is no consensus on the subunit composition of newly inserted receptors. Some studies have shown exclusive insertion of GluR1 (Thiagarajan et al., 2005; Sutton et al., 2006), whereas others have shown both GluR1 and GluR2 (O'Brien et al., 1998; Wierenga et al., 2005). These differences may reflect different scaling paradigms, or different synaptic populations in different culture systems. Another

interpretation is that the two findings represent two stages of synaptic scaling, similar to a model of LTP (Plant et al., 2006), in which GluR1 containing AMPARs are initially inserted and GluR2 containing AMPARs gradually replace them (Sutton et al., 2006). However, fewer studies have looked at the mechanisms of scaling down of synaptic strengths in response to increases in activity. Although recent work has shown that GluR2 and calcium influx through L-type calcium channels are necessary for scaling down in response to chronic photo stimulation (Goold and Nicoll, 2011), the precise mechanisms of AMPAR changes during scaling are unclear.

Homeostatic plasticity occurs on the timescale of days, and requires transcription (Ibata et al., 2008). In agreement with this line of reasoning, it has been shown that the immediate early gene Arc/Arg3.1 has been implicated in the scaling up of synaptic currents (Tzingounis and Nicoll, 2006). Other studies investigating synaptic scaling have implicated BDNF, TNFα, β3 integrin, MHC I and CaMKIV in scaling up of synaptic currents following silencing of neurons (Pozo and Goda, 2010). In contrast, much less is known about the regulation of scaling down in response to increases in activity and we wanted to determine what molecular mechanisms decrease synaptic strength following elevated activity. We postulated that the timescale of regulation would implicate transcription changes; therefore, we screened for genes upregulated during increases in activity. In Chapters 5 and 6, I will present data showing that the transcriptional repressor MeCP2, which was identified in the screen, is necessary for synaptic scaling and regulates the expression of the glutamate receptor subunit GluR2.

1.5 CONCLUSIONS

Concluding remarks

From previous studies, we know that axons can identify target-cell type and adjust presynaptic properties to suit their postsynaptic partners. It is clear that synaptic adhesion molecules represent a potential mechanism to induce synapse formation, and potentially confer synapse-specific properties. We reason that cell adhesion molecules are candidates for target-cell specificity since they are capable of transsynaptic interactions, and aim to identify what cell adhesion molecules are responsible for providing a target-derived cue for CA1 axons. Chapters 2 and 3 identify Elfn1 as a novel synaptic organizing protein and present experiments that describe the role of Elfn1 in short-term plasticity at CA1-OLM synapses. In Chapter 4, I will discuss the findings of Chapters 2 and 3 and their implication for a mechanism of target-cell specificity.

Cell adhesion molecules are a molecular mechanism that can generate synaptic diversity, but activity can also shapes neural circuits. Homeostatic plasticity of neural circuits enables synapses to adjust strength depending on overall activity levels. This plasticity is thought to keep firing rates within a manageable dynamic range, and we aim to identify what molecular mechanisms regulate this process. Chapter 5 presents a collaborative study with Dr. Zilong Qiu that addresses the role of MeCP2 in activity-dependent changes in synaptic strength. Conclusions based on these experiments are discussed in Chapter 6. Ultimately, neural circuits are shaped by molecular mechanisms that establish and diversify synapses, as well as by activity-dependent modification of those circuits. Both processes are needed to support a functional, plastic neural circuit capable of performing complex behavioral tasks.

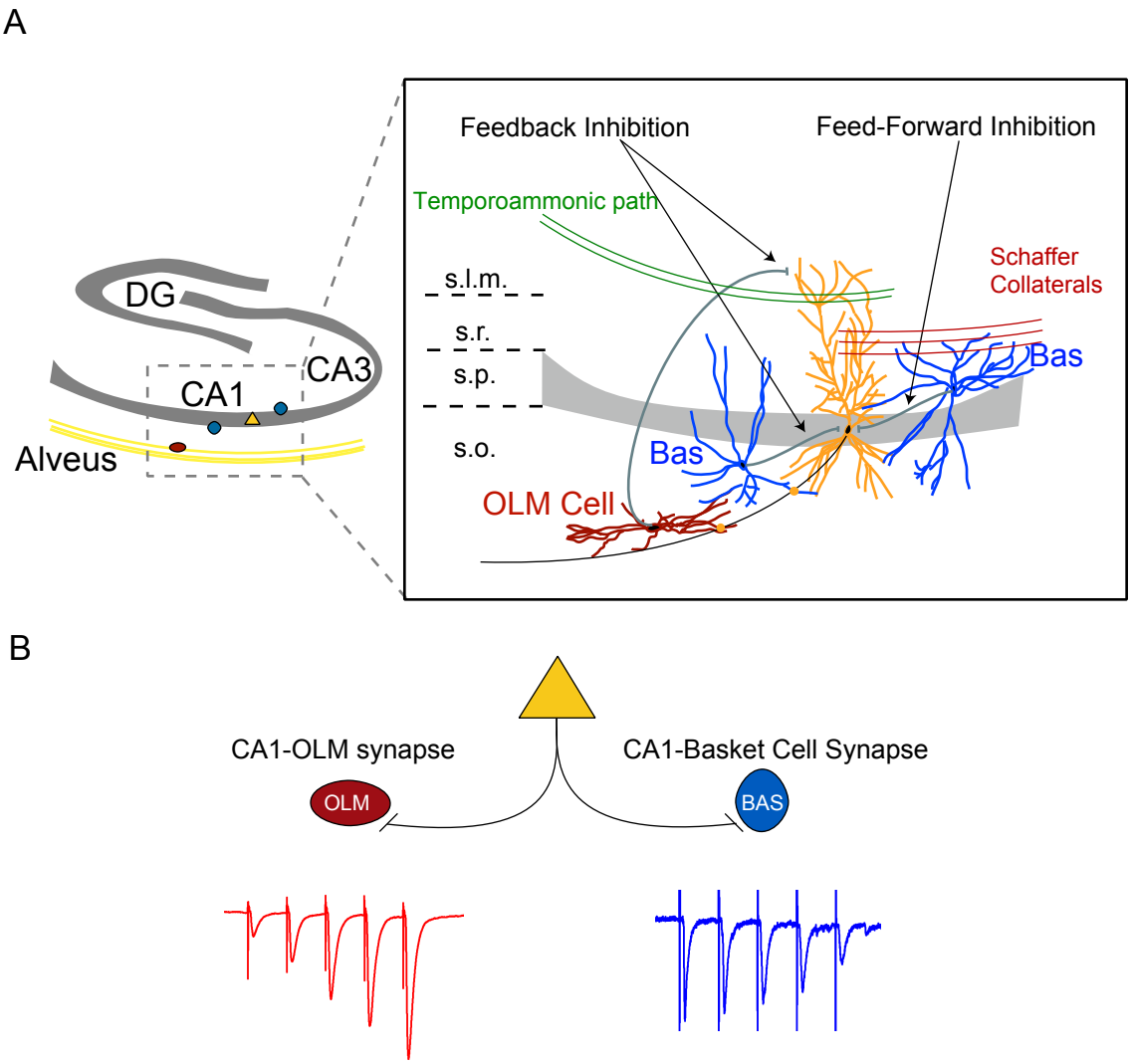

Figure 1.1 Hippocampal CA1 microcircuit

A. Schaffer collaterals (red axons) make excitatory synapses on CA1 pyramidal cells (yellow) as well as parvalbumin positive basket cells (blue) in the stratum radiatum (s.r.), which provide feed-forward inhibition. CA1 axons send divergent projections to different interneurons in the stratum oriens (s.o.). Basket cells (blue) provide strong feedback inhibition targeting the pyramidal cell somata. Oriens-lacunosum moleculare cells (OLM, in red) provide feedback inhibition that targets the distal dendrites of CA1 pyramidal neurons in the stratum lacunosum moleculare (s.l.m.).

B. CA1-OLM synapses exhibit short-term facilitation (red), whereas CA1-Basket cell synapses exhibit short-term depression (blue).

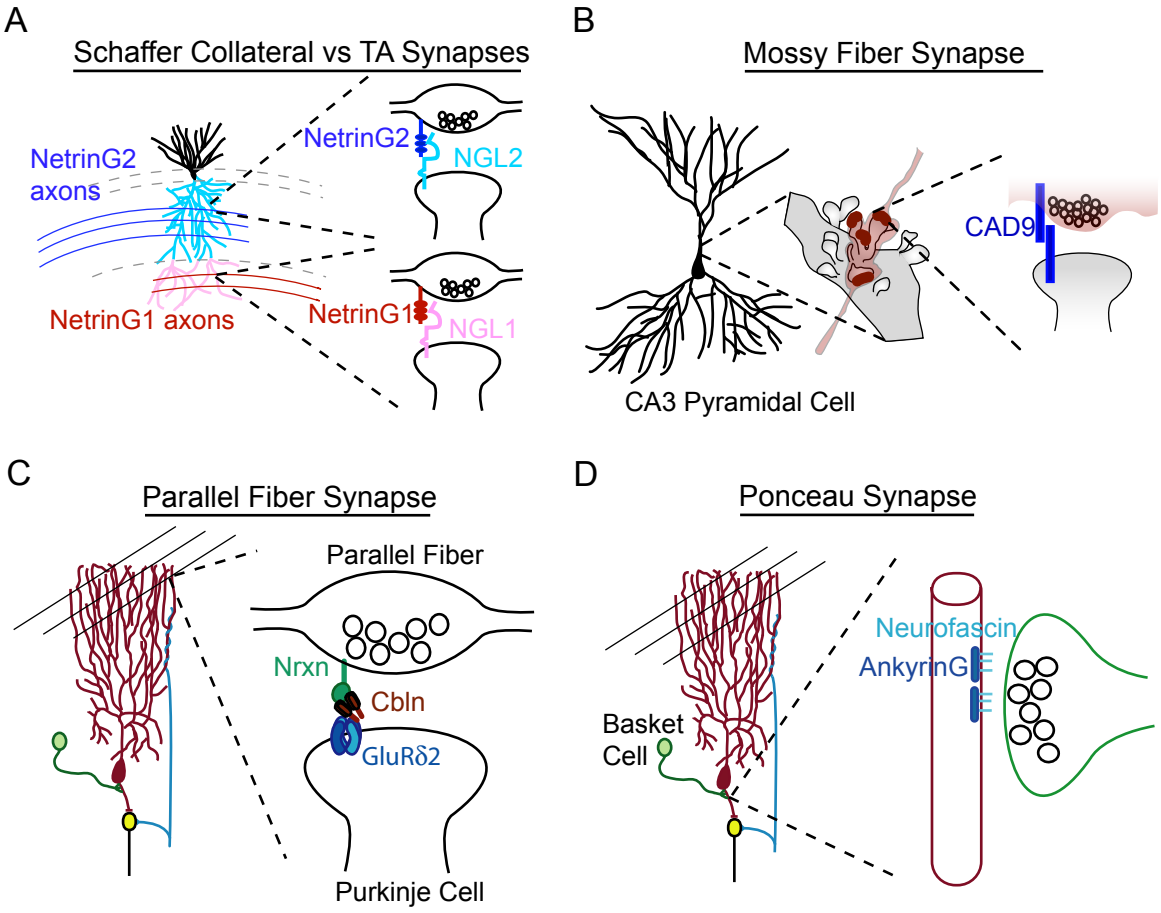

Figure 1.2 Cell adhesion molecules can be localized to specific synapses.

A. Schaffer collateral axons express Netrin G2, which binds to NGL2 on CA1 pyramidal cell dendrites, restricting it to the stratum radiatum. Temporoammonic axons from entorhinal cortex express Netrin G1, which binds to NGL1 on CA1 pyramidal cells, restricting it to the stratum lacunosum moleculare.

B. Mossy fiber terminals and CA3 pyramical cells express the cell adhesion molecule Cadherin-9. Cadherin-9 is required for the formation of a specialed synaptic structure, characterized by thorny excrescences and large presynaptic boutons.

C. GluRδ2 on Purkinje cells binds with Neurexin via a secreted intermediary, Cbln1.

D. Neurofascin and AnkyrinG postsynaptic complexes are required for the specific localization of basket cell axons terminals to the axon initial segment of Purkinje cells.

CHAPTER 2: CELL-TYPE AND SUBCELLULAR LOCALIZATION OF ELFN1

2.1 INTRODUCTION

The difference between CA1-OLM and CA1-PV synapses is just one example of the more general observation that synapses in the mammalian brain have diverse structural and physiological phenotypes that are essential for their proper function. It has been postulated that synaptic organizing molecules may play an instructive role in regulating the pre- and post-synaptic composition to fine tune synaptic properties (Mcmahon and Díaz, 2011). One family of proteins, leucine-rich repeat (LRR) proteins, exhibits many of the qualities of synaptic organizing molecules. They are a diverse class of transmembrane, membrane-associated, and secreted molecules unified by the presence of repeated leucine-rich motifs, which have been shown to act as protein-protein interaction domains (Dolan et al., 2007). LRR diversity has greatly expanded in mammals; the worm genome contains only 29 LRR-containing proteins whereas the mouse genome contains 135 (Dolan et al., 2007). Many of these proteins are expressed in the nervous system, often in strikingly specific patterns. Some have already been be localized to synapses and regulate synapse number, strength, or neurite growth, such as LRRTMS, NGLs, and SALMs (Linhoff et al., 2009b) (Kim et al., 2006) (de Wit et al., 2009a) (Ko et al., 2006). The functions of many others are completely unknown.

The size, diversity, and differential expression of the remaining members of the LRR superfamily suggest that these proteins may act as synaptic organizing molecules in non-overlapping populations of neurons, conferring unique physiological properties to particular sets of synapses. Since CA1 target-cell specificity requires a postsynaptic cue, and LRR proteins represent a potential mechanism for regulating specific synapses, I wanted to know if any LRR proteins were specifically localized to CA1-OLM synapses. To that end, I screened expression patterns of LRR-containing proteins to identify

candidates for CA1-OLM target cell specificity. Using hippocampal culture and immnohisotchemistry, I show that the LRR protein Elfn1 is specifically localized to excitatory inputs onto hippocampal OLM interneurons.

2.2 METHODS

Plasmids

The full length mouse clone for Elfn1 (Accession# BC059029) was obtained from Open Biosystems (Thermo Fisher Scientific, Huntsville, AL) and subcloned into the expression vector pEGFPN1 (Accession# U55762) to yield a C-terminal GFP fusion construct. The full length Elfn2 cDNA was cloned from mouse P7 cDNA and inserted into the pEGFPN1 plasmid to produce a C-terminal tagged Elfn2-GFP fusion construct.

In Situ Hybridization

In situ hybridizations were performed as described in (Pasterkamp et al., 1999), using 20 μm horizontal P7, P14, and P21 rat brain cryosections. Digoxigenin-labeled cRNA probes were generated from linearized cDNA templates. Full length mouse Elfn1 was subcloned in the reverse orientation into pcDNA3.1(-) to generate anti-sense riboprobes from the coding region using T7 RNA polymerase. For experiments combining in situ hybridization with immunohistochemistry, tissue was prepared using an immunoperoxidase detection kit prior to dehydration (Vectastain Elite ABC; Vector Labs, CA).

Hippocampal Culture

Hippocampal neurons were cultured from P0 Long-Evans rats (Charles River,

Wilmington, MA) and plated on poly-D-lysine (Millipore, Temecula, CA), and laminin (Invitrogen, Carlsbad, CA) coated chamber slides (Nalge Nunc International, Rochester, NY). Neurons were maintained in Neurobasal-A medium (Invitrogen) supplemented with B27, glucose, glutamax, and penicillin/streptomycin (Invitrogen).

Mixed-Culture Assay

Mixed-culture assays were performed as described in (Biederer and Scheiffele, 2007). HEK 293T cells were grown in DMEM (Invitrogen) supplemented with 10% FBS (Invitrogen) and penicillin/streptomycin. Cells were transfected with eGFP or Elfn1-GFP using Fugene6 (Roche). After 24 hours, cells were mechanically triturated and replated on hippocampal neurons (7 DIV) for 2 days and immunostained for synapsin and GFP.

Immunocytochemistry

Neurons were fixed at P14 in 4% paraformaldehyde in phosphate buffered saline (PBS) and processed for immunofluorescence according to standard procedures. For synapse density experiments, primary antibodies were: rabbit anti-VGlut1, rabbit anti-VGAT, mouse anti-gephyrin, (Synaptic Systems, Goettingen, Germany); mouse anti-PSD-95 (Affinity BioReagents, Rockford, IL); goat anti-GFP, chicken anti-Map2 (Abcam, Cambridge, MA). For mixed culture assay, primary antibodies were: rabbit anti-synapsin (Millipore) goat anti-GFP, (Abcam, Cambridge, MA). For cell type determination, primary antibodies were: mouse anti-GAD-6 (Developmental Studies Hybridoma Bank, Iowa City); mouse anti CamKII (Chemicon, Ramona, CA); rabbit anti-lrrc62 (Prestige Antibodies-Sigma, St. Louis, MO). Fluorophore-conjugated secondary antibodies were from Jackson ImmunoResearch (West Grove, PA) or Invitrogen. For post hoc morphological identification, slices were fixed overnight in 4%

paraformaldehyde in 0.1 M phosphate buffer (pH 7.4) following recordings. Tissue was prepared using an immunoperoxidase procedure (Vectastain Elite ABC; Vector Labs, CA) as described in (Cox et al., 1996).

Image Acquisition and Analysis

Images were captured on Leica SP5 confocal microscopes (Leica Microsystems, Bannockburn, IL). Z-stacks were collapsed in a maximum projection and analyzed using NIH ImageJ software. Images were thresholded using constant settings per experiment and the density of colocalizing pre- and postsynaptic puncta was measured per length of GFP-positive dendrite of transfected neurons. For quantification of mixed-culture assays, images were thresholded and the total area of synapsin puncta was measured and normalized to the total GFP-positive area per cell. For experiments to determine cell-type, z-stack images were collapsed and images were thresholded to determine colocalization of cell type markers. Fields of view at 20x were then counted for each cell type.

Mice

Somatostatin-IRES-Cre mice were created by the Huang lab, were provided by Massimo Scanziani are available through Jackson Labs. LSL CAG- tdTomato mice were created by the Allen Institute for Brain science and acquired from Jackson Labs.

2.3 RESULTS

Elfn1 is expressed in inhibitory interneurons

The diversity of synaptic phenotypes is likely to reflect a non-overlapping

expression of key synaptic organizing proteins, which differentially regulate the synaptic protein composition and give rise to unique synaptic properties. In order to screen for molecules involved in conferring specific properties on synapses onto interneurons, I used mRNA expression data from the Allen Brain Atlas to identify candidates. I postulated that these molecules would be synaptically localized and present in discrete populations of interneurons. They also are likely to be transmembrane proteins that could initiate contact across the synapse, a process that would require protein-protein interaction domains. We previously identified the leucine-rich repeat superfamily to contain many of these characteristics (de Wit et al., 2009a), and comprehensively screened the expression patterns of LRR-containing proteins in the Allen Brain Atlas for patterns that suggest restricted expression in interneurons.

A subfamily of LRR proteins, the Extracellular Leucine-rich fibronectin containing (Elfn) proteins have an expression pattern consistent with a role in cell type-specific synapse formation. Elfn1 shows strong and exclusive expression in interneurons, whereas, Elfn2 shows expression in the pyramidal cell layers in the hippocampus (Allen Mouse Brain Atlas). To confirm that Elfn1 and Elfn 2 were also differentially expressed during development, I performed in situ hybridization of rat brain sections at P7, P14, and P21 (Figure 2.1). During the second postnatal week, a time when hippocampal synapses are maturing, Elfn1 mRNA was restricted to scattered cells in the hippocampus, primarily located in the stratum oriens and hilus, whereas Elfn2 was expressed in the pyramidal cell layers. The expression pattern Elfn1 suggested and interneuron population, so I compared its expression to the expression of known interneuron markers. The striking similarity of Elfn1 expression to the expression of somatostatin (Sst), a marker for OLM interneurons encouraged me to focus on Elfn1 as a candidate for a target-derived cue in interneurons (Figure 2.2). To verify that individual

cells coexpress Elfn1 and Sst, I performed DIG-labeled in situ hybridization for Elfn1 mRNA followed by immunostaining for a marker of interneuron cell type. In transgenic animals with the reporter tdTomato under the control of either the Sst or parvalbumin (PV) promoters, I used an antibody to detect tdTomato-expressing cells (Figure 2.2). Horizontally oriented cells immediately adjacent to the alveus showed colabeling for Elfn1 mRNA and tdTomato protein in the Sst-tdTomato tissue, suggesting that Elfn1 was expressed in OLM interneurons. Elfn1 mRNA was not co-localized with PV/tdTomato neurons, indicating that Elfn1 was not expressed in basket cells. The selective expression of Elfn1 is Sst+ interneurons suggested that Elfn1 might regulate OLM-specific properties.

Elfn1 is localized to excitatory synapses

In order to examine the cellular and subcellular localization of Elfn1, I tested commercially available antibodies for binding specificity. An antibody generated to an Elfn2 peptide of a highly conserved domain between Elfn1 and Elfn2 recognized both Elfn1 and Elfn2 in HEK cells by immunofluorescence and Western Blot (Figure 2.3). However, in hippocampal cultures transfected with Elfn1-GFP or Elfn2-GFP, anti-Elfn immunoreactivity was selective for Elfn1, labeling only Elfn1-GFP expressing neurons (Figure 2.4). To confirm that this antibody was labeling the same cell-type as shown by in situ hybridization data, I cultured primary hippocampal neurons from P0 rat pups and immunostained them at 14 days in vitro (DIV) with anti-Elfn and CamKII or GAD-6 antibodies to label excitatory and inhibitory neurons, respectively. Elfn immunoreactivity was restricted to the dendrites of a subset of hippocampal neurons (Figure 2.5). In agreement with the colocalization in the combined in situ and immunostaining in hippocampal slices, these neurons expressed GAD-6, but not CamKII, and were Sst

positive (Figure 2.5). I found that almost all (97%) of the Elfn1 expressing cells contained Sst. Of all the Sst expressing cells, 69% expressed Elfn1 at levels detectable with the antibody, indicating that a majority of the Sst-expressing cells co-express Elfn1 (Figure 2.5). Sst -expressing CA1 interneurons in the stratum oriens correspond to orien-lacunosum moleculare (OLM) interneurons, which have horizontally oriented dendrites adjacent to the alevus and project to the stratum lacunosum moleculare. To confirm Elfn1 was expressed in OLM interneurons, I immunostained P14 rat sections with the anti-Sst and anti-Elfn antibodies (Figure 2.6). Elfn and Sst co-localize in the stratum oriens, especially in the outer oriens next to the alveus, supporting the notion that Elfn1 is located on the dendrites of Sst-positive OLM interneurons.

In order to determine if Elfn1 localizes to synapses, I immunostained dissociated hippocampal cultures for Elfn1 and looked at the colocalization of Elfn1 puncta with the glutamatergic and GABAergic postsynaptic markers PSD-95 and Gephyrin. Elfn1 puncta did not colocalize with gephyrin, but did overlap with a subset of PSD-95 puncta, suggesting that Elfn1 was restricted to excitatory synapses (Figure 2.7). These data, combined with the cell-type specific markers, imply that Elfn1 is localized to excitatory synapses onto Sst containing OLM interneurons.

Synaptogenesis is not regulated by Elfn1

Other leucine-rich repeat proteins have been shown to regulate synaptic density or synapse induction (Ko et al., 2006; de Wit et al., 2009a; Woo et al., 2009). Some synaptic molecules, such as Neuroligin, LRRTM2, or NGL2, when expressed in heterologous cells, will induce the formation of presynaptic terminals in contacting axons (Scheiffele et al., 2000; Kim et al., 2006; Linhoff et al., 2009a). Unlike LRRTM2 and NGL2, Elfn1 expressed in heterologous cells did not induce hemisynapses on contacting

axons, suggesting it is not involved in the induction of nascent synapses during development (Figure 2.8). To determine if Elfn1 has an effect on synapse number, I examined the effects of overexpressing Elfn1 in hippocampal cultures by transfecting an Elfn1-myc expressing plasmid at plating. Cells were fixed and stained at 14DIV for excitatory synapses using the excitatory synaptic markers PSD-95 and VGlut. Unlike in the overexpression of other synaptic molecules, I saw no effect of Elfn1 overexpression on synapse number (Figure 2.9). In parallel experiments, I recorded mEPSCs at 14 DIV from transfected cells to determine if there is a change in synaptic strength, but I see not an effect of Elfn1 overexpression on mEPSC amplitude or frequency, suggesting that it does not act as a synaptogenic molecule (Figure 2.10). These data imply that Elfn1 does not broadly regulate synapse formation or postsynaptic differentiation, but may exert a more selective role on synaptic properties, as expected from its restricted localization.

2.4 CONCLUSIONS

These observations identify Elfn1 as a novel synaptic protein that is specifically expressed in somatostatin interneurons in the hippocampus. Furthermore, it is restricted to excitatory synapses. Although we have not ruled out the possibility that Elfn1 may be at CA3-OLM synapses, the majority of excitatory input to OLM cells originates from CA1 axon collaterals, so is likely present at CA1-OLM synapses. Unlike many other synaptic LRRs, Elfn1 does not have an affect on synapse strength or number in vitro. This is not surprising. Since its expression is restricted to such a small subset of connections, it is more likely to play a role in establishing synapses between pyramidal cells and OLM interneurons, or in regulating synaptic properties that are unique to the CA1-OLM synapse. Although the heterologous coculture does not perfectly recapitulate the

development environment in vivo, I find that Elfn1 cannot induce synapses in this assay, suggesting that it does not function in establishing synapses. Instead, these findings strengthen the hypothesis that Elfn1 may be a target-derived cue that can regulate synapse-specific function. Chapter 3 investigates this possibility in experiments designed to determine the effect that loss of Elfn1 has on the function of CA1-OLM synapses.

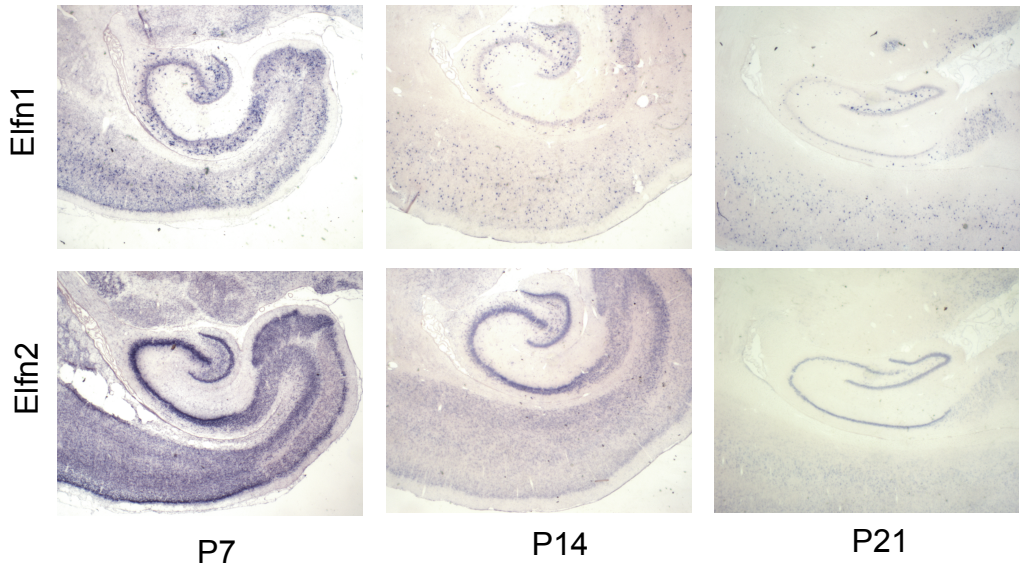

Figure 2.1 Elfn1 is expressed in the developing hippocampus

In situ hybridization on rat hippocampal sections using antisense probes for Elfn1 and Elfn2 at 7, 14, and 21 days postnatal. Elfn1 shows expression in scattered cells in the stratum oriens and hilus, whereas Elfn2 shows stronger signal in the pyramidal cell layers.

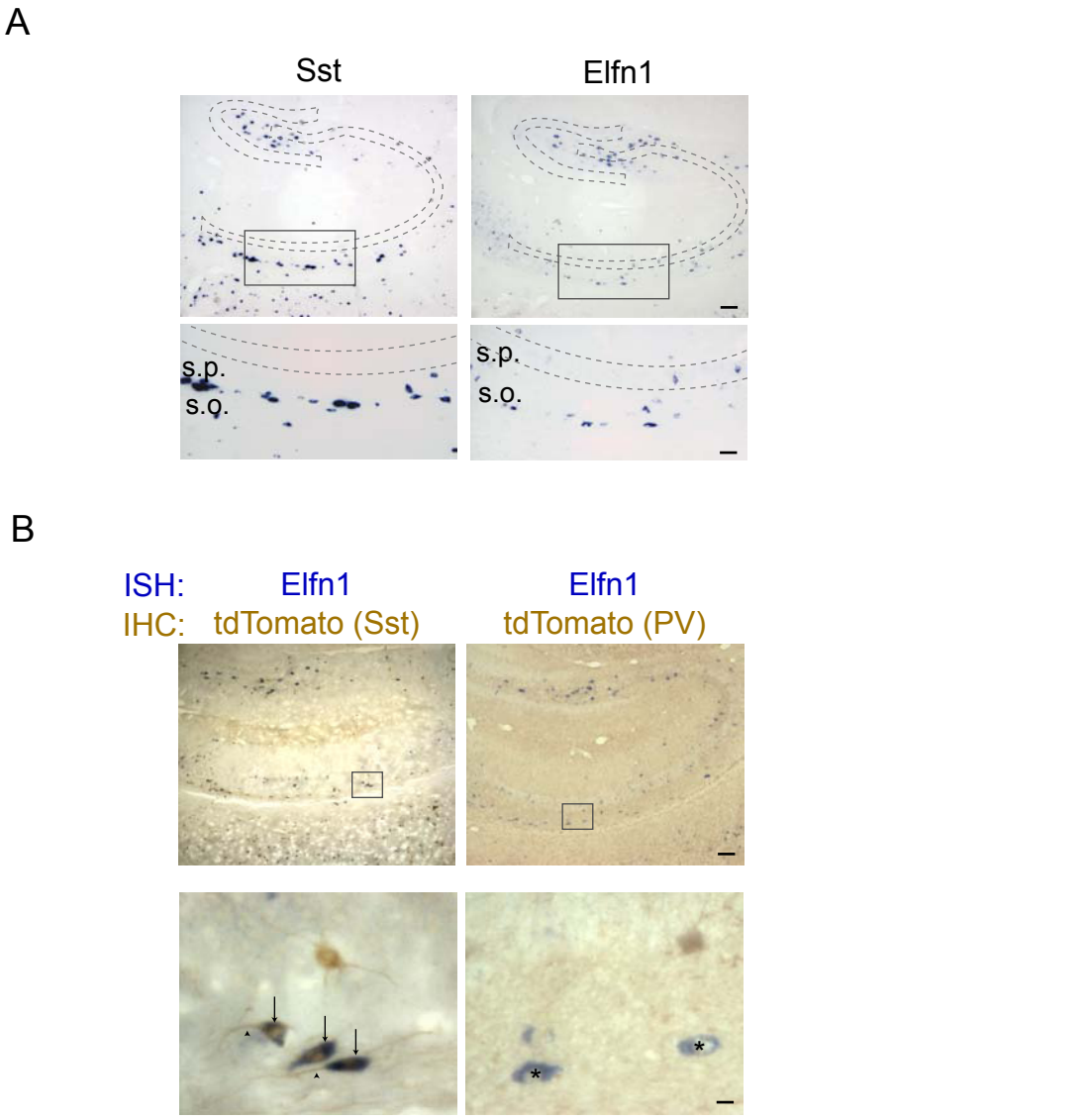

Figure 2.2 Elfn1 is expressed in hippocampal somatostatin containing inhibitory interneurons.

A. In situ hybridization (ISH) on mouse sections with antisense probes to somatostatin and Elfn1; scale bar = 25µm. Lower panels, magnified view of stratum oriens from sections above; Scale bar = 2.5µm. Dotted lines indicate borders of pyramidal and granule cell layers.

B. In situ hybridization for Elfn1 (blue precipitate) combined with immunostaining for tdTomato with DAB detection (brown precipitate) to determine colocalization with inter-neuron types in two reporter lines, somatostatin(Stt)-tdTomato and parvalbumin(PV)-tdTomato. Precipitates colocalize in peri-alvear cells in Sst-tdTomato somata (arrows) and proximal dendrites (arrowheads) but not PV-tdTomato tissue (asterisk). Proximal dendrites of labeled cells show horizontal morphology. Upper scale bar = 25µm; lower scale bar = 2.5 µm.

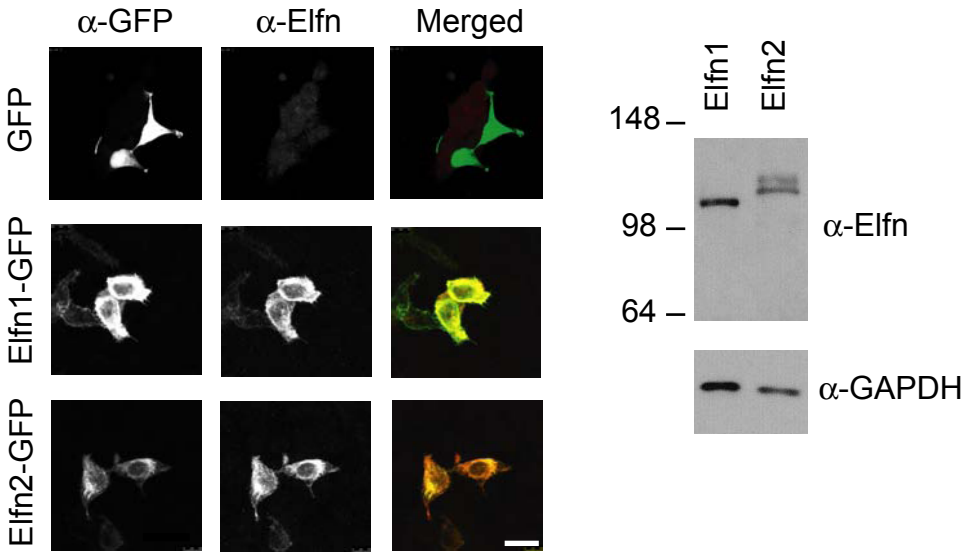

Figure 2.3 Anti-Elfn recognizes Elfn1 and Elfn2 in HEK Cells

Left, HEK cells transfected with GFP control, Elfn1-GFP or Elfn2-GFP and immuno-stained using an antibody that recognizes Elfn1 and Elfn1. Right, western Blot of HEK cell lysates expressing Elfn1 and Elfn2, blotted using α-Elfn and α-GAPDH antibodies. Scale bar = 20μm.

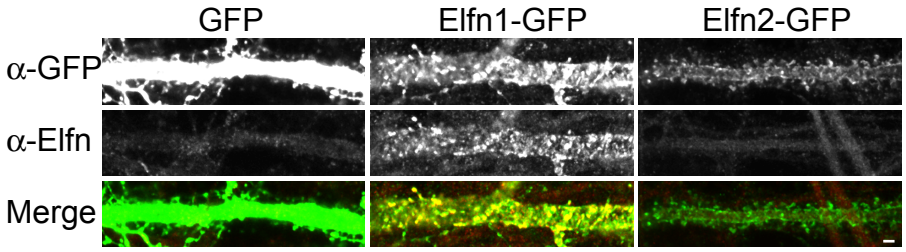

Figure 2.4 Anti-Elfn antibody preferentially recognizes Elfn1 in neurons.

Neurons overexpressing Elfn1-GFP and Elfn2-GFP stained with the α-Elfn antibody, which preferentially recongnizes Elfn1 in culture. Elfn2 expressing dendrites show little immunoreactivity, Scale bar = 2μm.

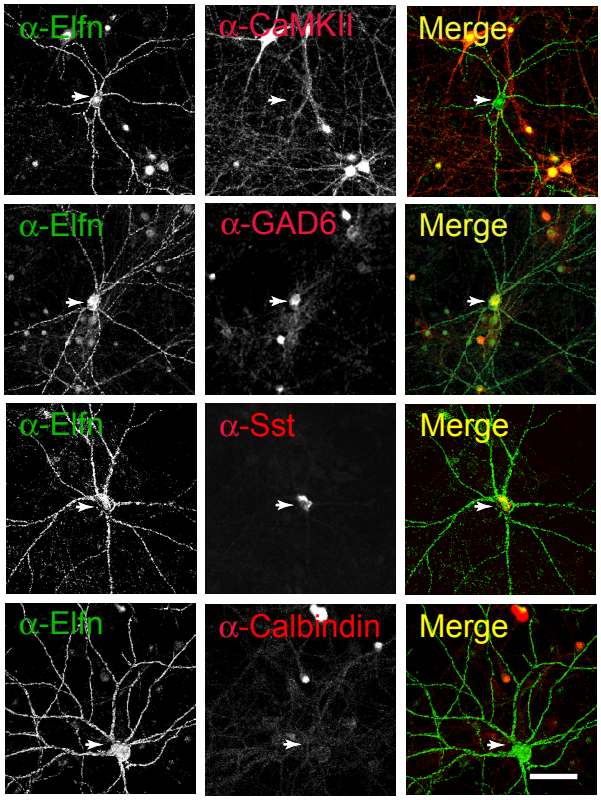

	GAD	CamKII	Sst	Calb
% of Elfn+ cells with marker	97	0	96	0
% of each cell type with Elfn	18	0	69	0

Figure 2.5 Elfn antibody immunoreactivity is restricted to somatostatin interneurons in dissociated hippocampal cultures.

Dissociated hippocampal cultures at 14DIV fixed and immunostained for Elfn and either CamKII, GAD-6, somatostatin, or calbindin. Table, quantification of the proportion of Elfn expressing cells that co-express either CamKII, GAD-6, somatostatin or calbindin (Top row) and the proportion of cells expressing either CamKII, GAD-5, somatostatin or calbindin that co-express Elfn (Bottom row). Scale bar = 20μm.

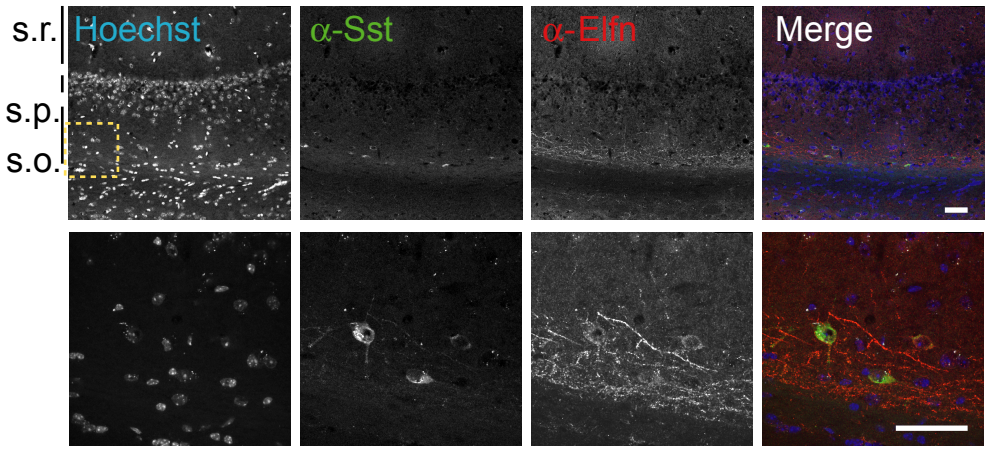

Figure 2.6 Elfn antibody immunoreactivity is enriched in the stratum oriens.

P14 rat hippocampal sections stained for Elfn, somatostatin, and Hoechst. Upper panels, low magnification images of CA1. Lower panels, high magnification images of CA1 oriens area from dotted box above. Scale bars = 20μm.

A

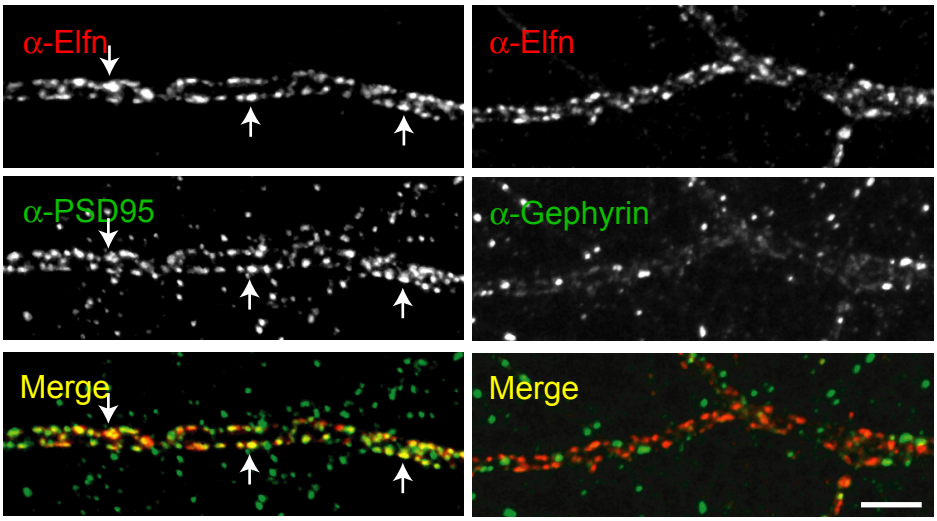

B

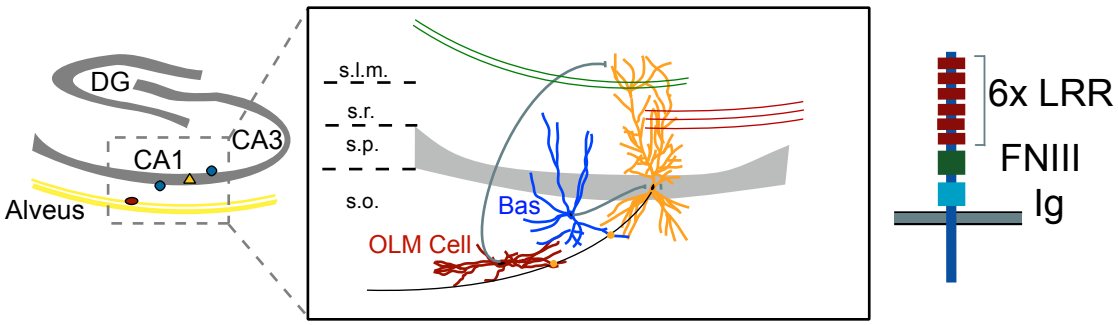

Figure 2.7 Elfn1 is localized to excitatory synapses on OLM interneurons

A. Dendrites in a dissociated hippocampal cultures stained for Elfn and the excitatory postsynaptic marker PSD95 or the inhibitory postsynaptic marker gephyrin. Scale bar = 5μm.

B. Left, model of Elfn1 localization to excitatory CA1 inputs to somatostatin positive oriens interneurons. These provide feedback inhibition to the CA1 pyramidal cells. Right, schematic domain organization of Elfn1. Lrr, Leucine-rich repeat; FNIII, Fibronectin Type III domain; Ig, Immunogobulin domain.

A

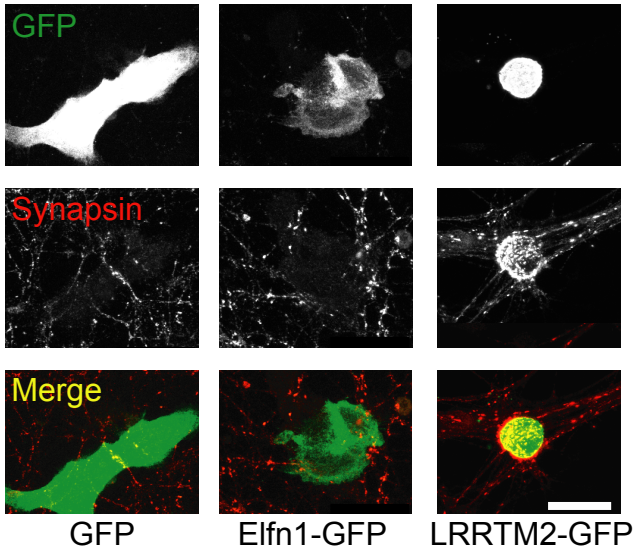

B

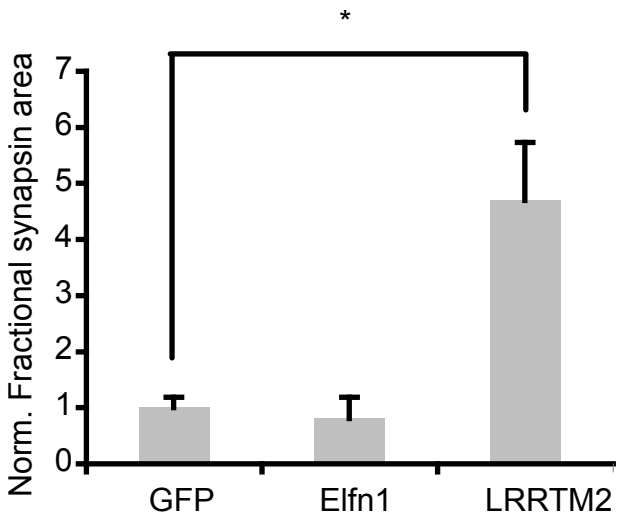

Figure 2.8 Elfn1 is not a synapse inducing molecule.

A. HEK cells expressing GFP, Elfn1, or LRRTM2 are cocultured with dissociated hippocampal neurons, from 7-9 DIV, fixed and stained for synapsin.

B. Fractional area of the HEK cell stained with synapsin, normalized to the GFP control transfected cells. Asterisk indicate $p<.05$, Scale bar is 20μm. Error bars represent SEM.

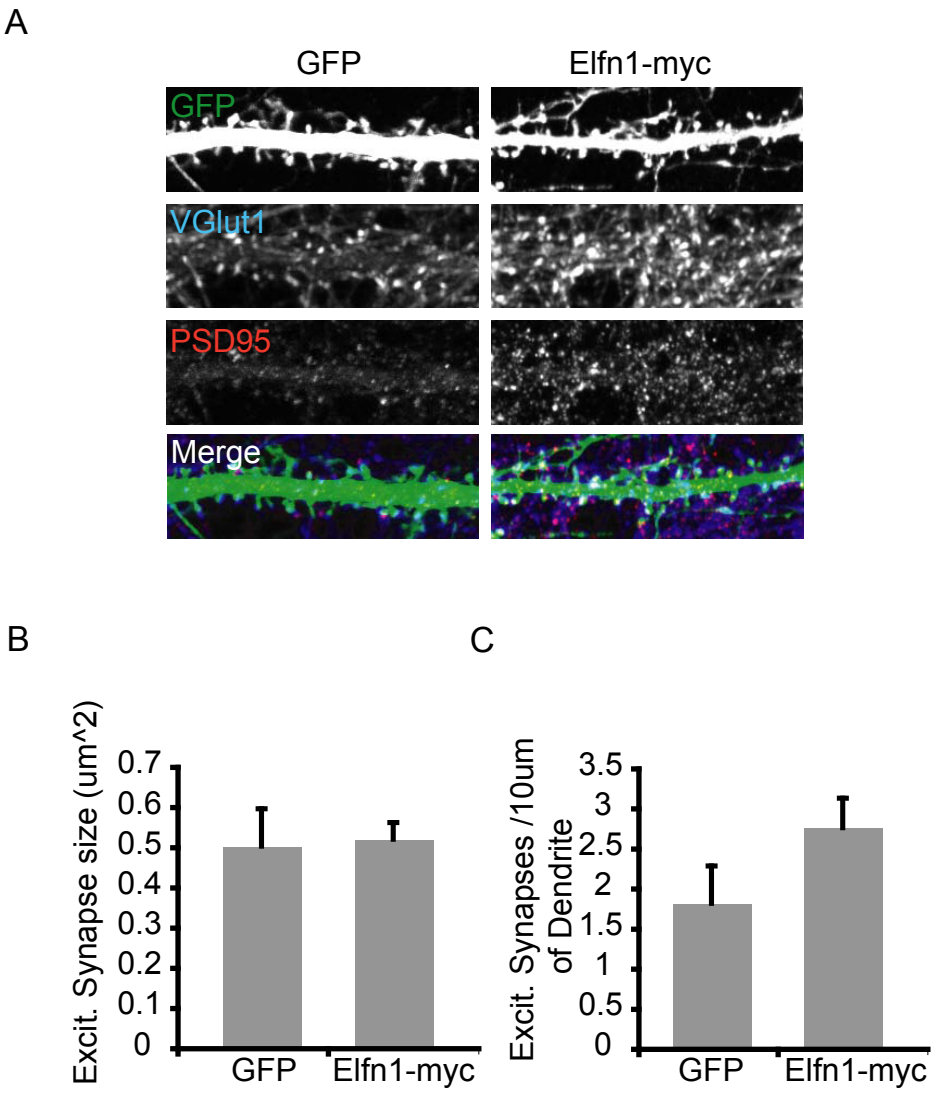

Figure 2.9 Elfn1 overexpression does not alter synapse density

A. Neurons were electroporated at plating with GFP and Elfn1 and fixed at 14DIV. Left, neurons were stained for Vglut and PSD95 to visualize excitatory synapses at 14DIV.

B. Quantification excitatory synapse size.

C. Quantification excitatory synapse density.

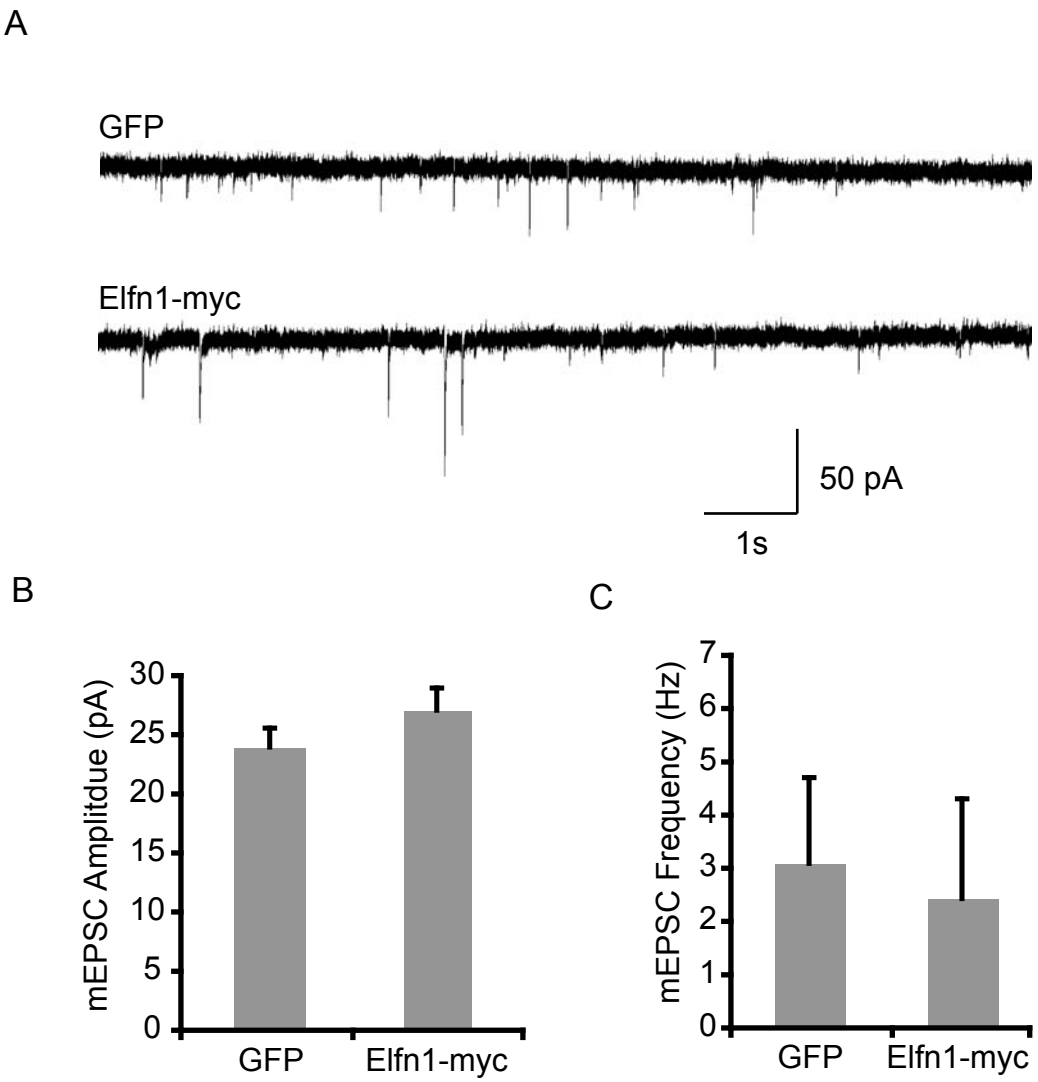

Figure 2.10 Elfn1 overexpression does not affect synapse strength

A. Example traces of mEPSCs recorded at 14DIV in the presence of gabazine, APV and TTX to isolate AMPA-mediated currents.

B. Quantification of mEPSC amplitude.

C. Quantification of mEPSC frequency.

CHAPTER 3: ROLE OF ELFN1 IN HIPPOCAMPAL SHORT-TERM PLASTICITY

3.1 INTRODUCTION

Inhibitory circuits in the hippocampus play an important role in shaping hippocampal activity and can be broadly divided into feed-forward and feedback circuits. In the CA1 region of the hippocampus, feedback inhibition consists of recurrent CA1 pyramidal cell axon collaterals synapsing onto local inhibitory interneurons (Andersen et al., 1963). CA1 collaterals impinge on different types of GABAergic interneurons, including basket cells and oriens-lacunosum molecule (OLM) interneurons (Lacaille et al., 1987; Ali et al., 1998; Ali and Thomson, 1998) (Figure 1.1). Recruiting each of these inhibitory cell types results in feedback inhibition with unique attributes. A strong, but rapidly depressing, synapse onto basket cells serves to determine a window of coincidence detection by engaging inhibition quickly and transiently (Ali et al., 1998; Pouille and Scanziani, 2004). Basket cells in turn form inhibitory synapses on pyramidal cell somata, providing strong, transient somatic inhibition. In contrast, CA1 synapses onto OLM interneurons are strongly facilitating and provide feedback inhibition to distal CA1 dendrites (Ali and Thomson, 1998). The late-onset, but strongly facilitating nature of this synapse engages the CA1-OLM inhibitory circuit only after repetitive activity in pyramidal cells, making this circuit function as an integrator of hippocampal activity (Pouille and Scanziani, 2004). The fact that single CA1 axons form functionally distinct synapses onto basket and OLM cells suggests that a target-derived cue is necessary to communicate postsynaptic identity to the contacting axon. However, molecules that regulate these synapse-specific properties have not been identified.

In this study, I investigate the role of leucine-rich repeat (LRR) proteins in regulating synapse specific functional properties in the hippocampal CA1 circuit. LRR proteins are a diverse class of transmembrane, membrane-associated, and secreted

molecules, some of which have been shown to have spatially restricted expression patterns and synaptic localization (Kobe and Kajava, 2001; Kim et al., 2006; Ko et al., 2006; Dolan et al., 2007; de Wit et al., 2009a; Linhoff et al., 2009a; de Wit et al., 2010). Here I show that the LRR protein Elfn1 is required for short-term facilitation of the CA1 pyramidal cell input.

3.2 METHODS

Plasmids

For knockdown experiments, an shRNA was obtained from Open Biosystems targeting nucleotides 2440-2460 of Elfn1 (gacatcctagactactggaaa), which is 100% conserved between mouse and rat. The U6 promoter and shRNA was subcloned into the lentiviral plasmid FUGW (Addgene), which contains a ubiquitin promoter driving eGFP expression. The Elfn1 rescue construct had a single point mutation in the shRNA target sequence (gacatccttgactactggaaa).

Lentivirus Production

For lentivirus production, 293T cells were transfected with control or shLRRTM2 containing FCK(0.4)GW vector plasmids and helper plasmids MDL, RSV-REV and VSVG using polyethylenimine (PEI). Supernatant was collected 48 hrs after transfection, spun at 2000 rpm to remove debris and filtered through a 0.22 μm filter (Millipore). Viral particles were pelleted using two centrifugation steps at 19500 rpm for 2 hrs each. The final pellet was resuspended in 100 μl PBS and stored at -80°C in 10 μl aliquots.

Electrophysiology

Postnatal day 5-6 mouse pups from Som-IRES-Cre x LSL tdTomato mice were anaesthetized with isoflurane and received a subcutaneous injection of bupivacaine. Lentivirus injections were targeted to the CA1 region of the hippocampus using stereotaxic coordinates. At Postnatal day 13-16, 300 μm slices were maintained in a sucrose substituted solution: 83 NaCl, 2.5 KCl, 1 NaH_2PO_4, 26 $NaHCO_3$, 22 glucose, 72 sucrose, 0.5 $CaCl_2$, 3.3 $MgCl_2$. Slices were moved to the recording chamber and perfused with an ACSF that consisted of (in mM): 119 NaCl, 2.5 KCl, 26 $NaHCO_3$, 1 NaH_2PO_4, 2 $MgCl_2$, 2 $CaCl_2$, 11 glucose, 0.1 picrotoxin and bubbled constantly with 95% O_2/5% CO_2. Somatostatin positive oriens interneurons were visualized by infrared differential interference and tdTomato and eGFP epifluorescence microscopy (Zeiss Axioskop 2). Whole-cell voltage clamp recordings were made under visual guidance from neurons lying near the alveus that expressed both eGFP and tdTomato using ~3MΩ pipettes pulled on a horizontal micropipette puller (Sutter P-97) and filled with an internal solution that contained (in mM): 130 Cs-methanosulfonate, 5 NaCl, 10 EGTA, 10 HEPES, 10 phosphocreatine, and 2 Mg-ATP, pH 7.3 with CsOH, 280-290 mOsm. Synaptic responses were evoked every 15 s with a bipolar cluster electrode (FHC) placed in the alveus above the most distal portion of the subiculum. A glass recording pipette was placed in the alveus immediately adjacent to the infected cell to record the fiber volley following stimulation. The signals were low-pass filtered at 2 kHz, and digitized at 10 kHz (Molecular Devices Multiclamp 700B) and analyzed with pClamp 9 (Molecular Devices). Series resistance (Rs) and input resistance (Rin) were monitored throughout the experiment by measuring the capacitative transient and steady state deflection in response to a -5 mV test pulse, respectively.

Short-term facilitation was measured at a holding potential of -70mV by delivering a train of 5 stimuli at 5, 10, 20, and 40 Hz. At least 10 sweeps were averaged at each frequency and the amplitude was calculated as the average 1 ms around the peak. The amplitudes were normalized to the amplitude response to the first stimulus in a train to determine the facilitation ratio. To compare evoked responses across animals, the first EPSC for each train was normalized to amplitude of the fiber volley. To determine rectification of synaptic currents, D-APV (50μM) was added to the perfusion solution. The alveus was stimulated once, as described above and then the holding potential was increased from 70mv to +70 mV by 20 mV increments, and repeated 10 times to calculate an average. For MK801 experiments, DNQX (20μM) was used to block non-NMDA currents. The cell was held at +40mV and after a steady baseline was attained, MK801 (40μM) was washed in and the alveus was repetitively stimulated at 5 s intervals.

3.3 RESULTS

Elfn1 is required for short-term facilitation at CA1-OLM synapses.

OLM interneurons are unique in that they receive highly facilitating excitatory input from pyramidal neurons (Lacaille et al., 1987). In light of the specific restriction of Elfn1 to this class of synapses, I wanted to determine if Elfn1 regulates the synapse-specific short-term plasticity in OLM neurons. To this aim, I examined the functional consequence of knocking down Elfn1 expression in Sst+ interneurons using an shRNA targeting Elfn1. The construct was validated in HEK cells coexpressing the shRNA and GFP tagged Elfn1. The shRNA efficiently reduced Elfn1 protein levels (Figure 3.1). This could be rescued by a single point mutation in the target sequence. Furthermore, the shRNA did not alter levels of Elfn2.

To identify OLM interneurons, I crossed a somatostatin-IRES-Cre mouse line with a CAG LSL tdTomato mouse line, which produced a line with tdTomato labeling all Sst positive cells (Figure 3.1). At P6, shElfn1 lentivirus or control virus expressing GFP was injected into the CA1 region of these mice, and at P13-16 acute hippocampal slices were prepared for electrophysiological recordings. In these mice, the Sst+ neurons are labeled red and the Elfn1 shRNA infected neurons are labeled green (Figure 3.2). The majority of excitatory input onto Sst-containing oriens interneurons originates from CA1 collaterals, which exit the hippocampus via the alveus (Blasco-Ibafiez and Freund, 1995). I used distal alvear stimulation to selectively stimulate these axons (Lacaille et al., 1987) and recorded from tdTomato positive, GFP infected cells (Figure 3.2).

To determine if Elfn1 was required for short-term facilitation at CA1-OLM synapses, I delivered 5 stimuli at 20Hz with an electrode placed in the alveus and recorded the evoked EPSC using whole-cell voltage clamp. Control GFP-infected Sst+ neurons showed a strong facilitation to alvear stimulation as expected (Figure 3.2). In contrast, short-term facilitation at the CA1-Sst interneuron synapse was markedly reduced in neurons expressing the Elfn1 shRNA (Figure 3.2). The facilitation ratio, defined as the ratio of the fifth stimulus to the first, was reduced by 40% after lentiviral-mediated knockdown of Elfn1. This deficit in short-term facilitation was seen across at 20 and 40 Hz, suggesting that Elfn1 regulates short-term facilitation across a range of physiologically relevant input frequencies (Figure 3.3).

Elfn1 knockdown reduces synaptic strength

To determine if Elfn1 knockdown changes the synaptic strength of CA1 inputs onto OLM neurons, I normalized the evoked response OLM cells to the amplitude of the fiber volley recorded using a field electrode in the alveus immediately adjacent to the

recorded cell. While these experiments showed that Elfn1 knockdown increased the evoked response amplitude, the variability in the fiber volley to EPSC amplitude relationship led us to reason that it did not adequately normalize for stimulus intensity (Figure 3.4).

To better address the possibility of a change in evoked amplitude, I adapted a technique that has been used successfully at other synapses to compare the inputs onto neighboring infected and uninfected neurons (Zhu et al., 2000) . I recorded simultaneously from two cells, both identified by tdTomato epifluorescence and one also expressing GFP from lentiviral infection (Figure 3.5). I measured the evoked EPSC amplitude from stimulation of the alveus and compared amplitude in simultaneously recorded cells, plotting infected amplitude against uninfected control cell amplitude. Neighboring Sst interneurons show some variability, but across the population the mean amplitudes are the same, as seen in the GFP control where the average lies near the unity line. In contrast, Elfn1 knockdown neurons showed an increase in the evoked response when compared to simultaneously recorded neighboring cells, suggesting that endogenous Elfn1 normally restricts the strength of the evoked response.

Elfn1 regulates facilitation by a presynaptic mechanism

The effects of Elfn1 knockdown on short-term plasticity and synapse strength could both be due to either pre- or postsynaptic changes. An increase in release probability would increase the initial evoked EPSC amplitude, but would also result in a more rapid depletion of the readily-releasable pool, limiting the facilitation at the synapse, in agreement with our previous results. To determine if the change in facilitation was the result of a presynaptic change in probability of release, I repeatedly stimulated the alveus in the presence the use-dependent NMDAR antagonist MK801

(DNQX was added to the bath to isolate NMDAR currents.) Since MK801 blocks NMDA receptors in a use-dependent manner, synapses that have a higher probably of release will release glutamate more often and NMDARs at those synapses will be blocked more quickly (Rosenmund et al., 1993). The decay of the NMDA current was normalized to the initial amplitude and plotted over stimulus number to determine the time course of NMDA block (Figure 3.6). Neurons infected with the lentivirus containing Elfn1 shRNA showed a faster block of NMDA EPSCs compared to control infected neurons (Figure 3.6), verifying that Elfn1 knockdown results in an increase in release probability. An increased probability of release could explain both the larger evoked response, since a higher proportion of synapses would release, and the reduced short-term facilitation, resulting from depletion of the readily releasable pool.

Elfn1 does not regulate postsynaptic properties

While these experiments strongly suggest a presynaptic effect, they do not preclude the possibility that shElfn1 also triggers postsynaptic changes. To determine if Elfn1 regulates postsynaptic responses, I measured the ratio of synaptic AMPAR- to NMDAR-mediated currents by recording at -70mV and subsequently at +40mV in the presence DNQX and detected no effect of Elfn1 knockdown on AMPA/NMDA ratio (Figure 3.7). Similarly, the decay kinetics of the AMPAR and NMDAR mediated components was unchanged (Figure 3.7). CA1-Sst interneuron synapses are known to contain a high proportion of GluR2 lacking, inward-rectifying AMPA receptors (Croce et al., 2010). To test the rectification of these synapses, I recorded the evoked response to alvear stimulation at different holding potentials and plotted the voltage-current relationship. The rectification index is defined by the ratio of a line fit to the curve at holding potentials of 0mV to +70 mV to a line fit to the curve at -70mV to 0mV. The

rectification was not significantly different between control neurons and neurons infected with Elfn1 shRNA, indicating that that Elfn1 knockdown does not affect the proportion of GluR2 lacking AMPARs (Figure 3.8). Thus, basic postsynaptic properties are largely unaffected by Elfn1 manipulation.

A change in facilitation at this synapse has implications for the temporal dynamics of OLM spiking during CA1 activity. To test this, I performed simultaneous cell-attached recordings from neighboring infected and uninfected OLM neurons. A train of 10 stimuli at 20Hz was delivered to the alveus and the probability of OLM neuron spiking after each stimulus was calculated. As previously demonstrated, OLM neurons have a higher probability of spiking at later stimuli in the train under control conditions and more jitter than spikes evoked at CA1-PV synapses (Figure 3.9). When compared to control conditions, shElfn1 infected neurons show a higher spike probability at earlier stimuli in the train, in agreement with the observation that the initial underlying currents are larger following Elfn1 knockdown. Elfn1 knockdown shifts the short-term plasticity and spiking dynamics of the infected cell closer to that of CA1-basket cell synapses, which are recruited at the onset of activity. We wanted to know if we could likewise change short-term plasticity at CA1-basket cell synapses with Elfn1 overexpression, converting them to CA1-OLM-type synapses. We used lentiviral-mediated overexpresision of Elfn1-GFP in PV-IRES-Cre x LSL tdTomato mice to investigate changes in synaptic properties. The diffuse signal of GFP-tagged Elfn1 made it difficult to identify the infection of individual cells. The rate of infection near the injection site, where overexpression is the greatest, was high and resulted in a GFP haze in the neuropil where individual infection was difficult to discern. To maximize the probability of recording from a highly overexpressing PV cells, we selected cells in the middle of the infected area, assuming they too would be infected. For these PV cells, Elfn1

overexpression resulted in a switch from moderate short-term depression to short-term facilitation at 20Hz (Figure 3.10). Facilitation did not reach levels comparable to OLM synapse, so other competing cues may be present at CA1-PV synapses to increase transmitter release. Nonetheless, these data demonstrate that postsynaptic expression of Elfn1 is sufficient to alter presynaptic release probability and provide a retrograde, postsynaptic cue that regulates target-cell specificity.

3.4 Conclusions

Taken together, these results demonstrate that Elfn1 plays a key role in regulating facilitation of CA1-OLM synapses. Elfn1 is specifically localized to excitatory synapses onto somatostatin-expressing inhibitory interneurons in the stratum oriens. Knockdown of Elfn1 reduces short-term facilitation at this synapse and increases the evoked EPSC amplitude. MK801-dependent block of CA1-OLM transmission verifies that Elfn1 knockdown affects synapse function by a presynaptic mechanism. Moreover, loss of Elfn1 has no effect on several postsynaptic properties such as EPSC kinetics, AMPA/NDMA ratio, and rectification, but instead specifically affects presynaptic function.

These data demonstrate the postsynaptic Elfn1 is required for target-cell dependent modification of presynaptic release (Figure 3.11). It will be interesting to confirm that postsynaptic Elfn1 is sufficient to create a facilitating synapse. Preliminary experiments in PV basket cells show that this may be true, although there are likely competing mechanisms in PV basket cells that prevent a complete switch to strong facilitation. In light of the strong and specific effect on facilitation, it will be interesting to determine what the presynaptic binding partner is and by what mechanism their binding affects presynaptic release.

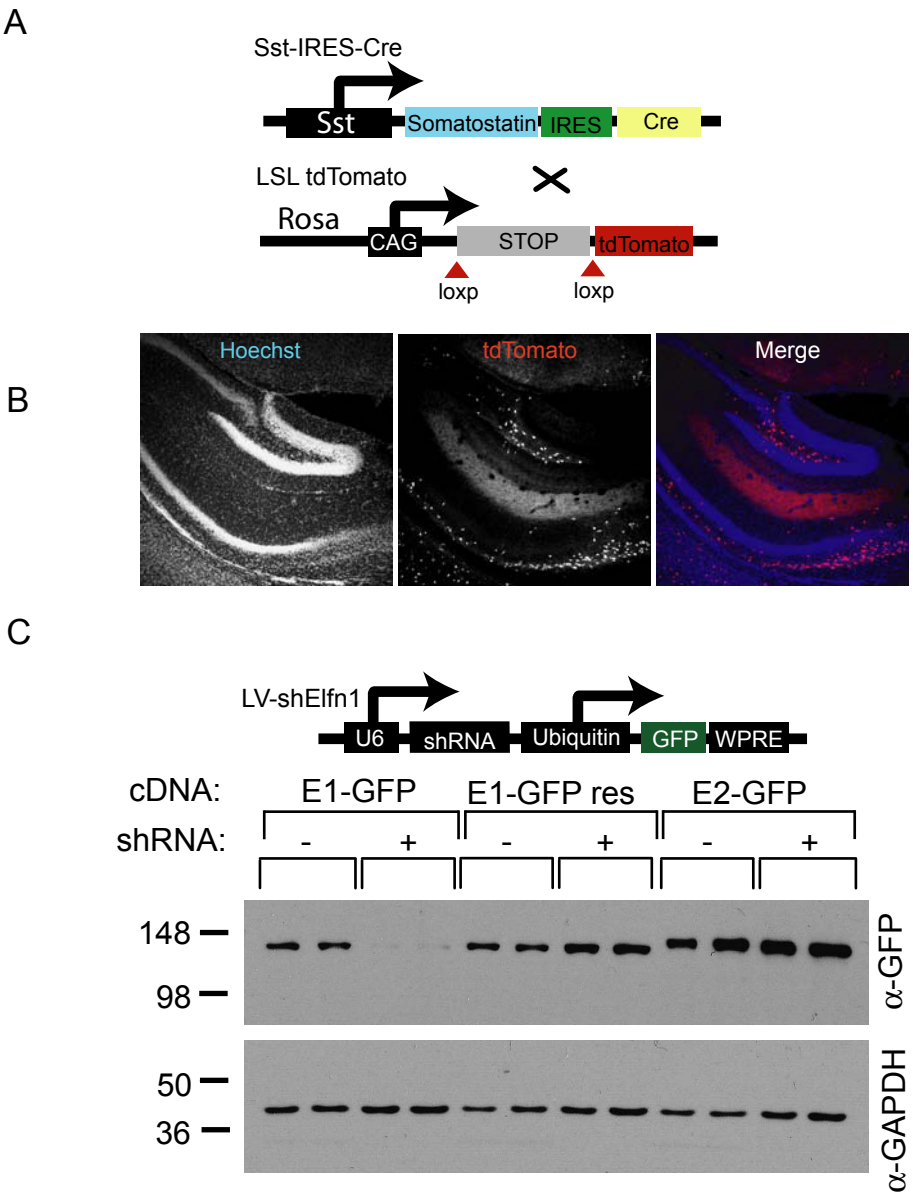

Figure 3.1 Targeting and manipulating Elfn1 expressing cells

A Left, Schematic of genetic cross labeling somatostatin containing interneurons *in vivo*.

B. Hoechst staining of hippocampal slices from SomiCre x tdTomato mice.

C. Western blot of HEK cell lysate from cells expressing Elfn1-GFP fusion construct cotransfected with control vector or vector containing shRNA targeting Elfn1, blotted GFP and GAPDH. Knockdown is rescued by a single point mutation (Elfn1-GFP res) in the target sequence of the Elfn1-GFP cDNA .

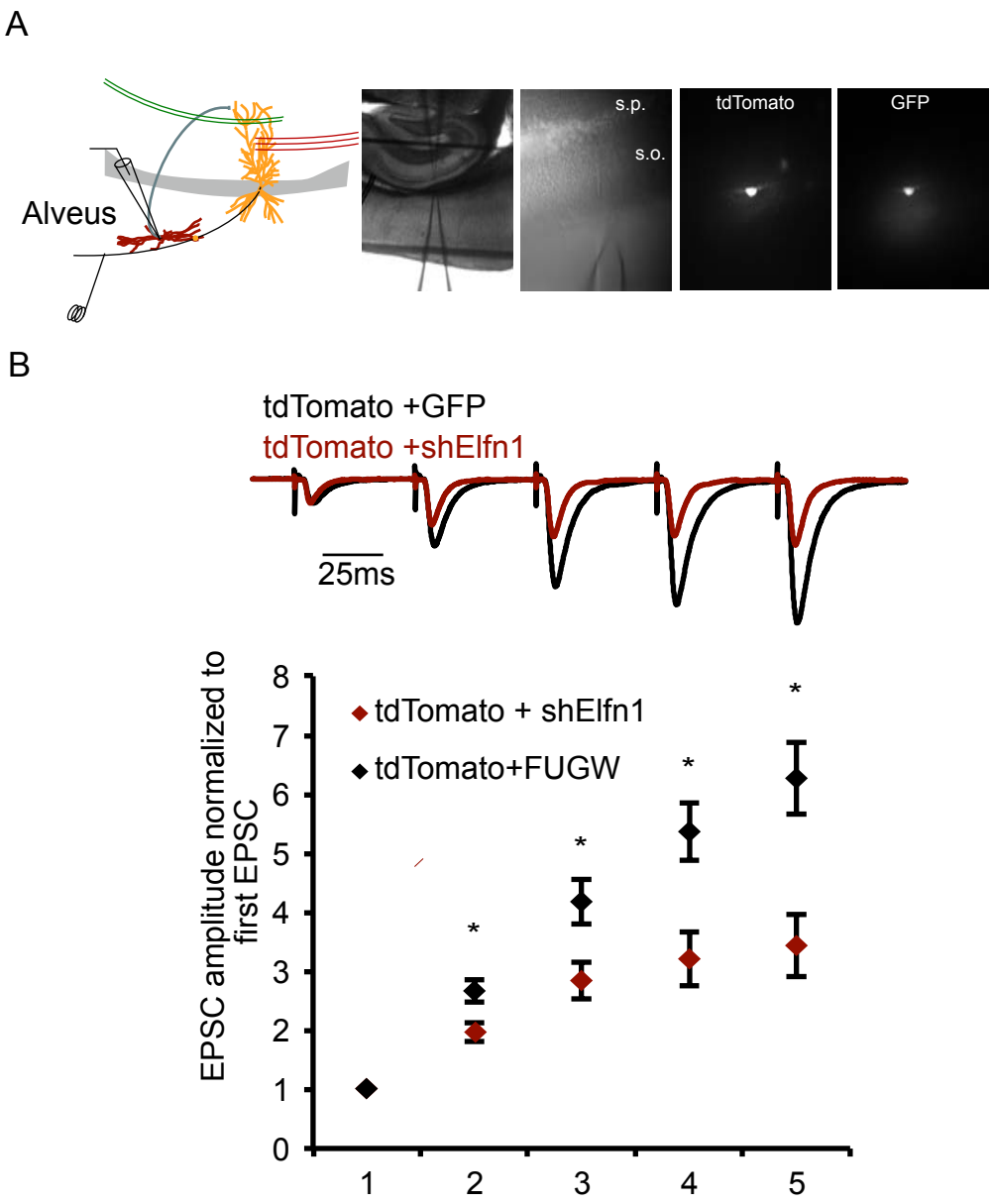

Figure 3.2 Elfn1 knockdown reduces short-term facilitation at CA1-OLM interneuron synapses.

A. Left, schematic of recording configuration for targeting CA1 inputs to oriens interneurons. Right, DIC images of recording setup and epifluorescene images of genetically encoded tdTomato and virally delivered GFP to target knockdown neurons for recording.

B. Top, postsynapic response of an example cell to 5 stimuli of the alveus at 20Hz, normalized to the first EPSC amplitude. Black, GFP control; red, shElfn1. Bottom, population data for EPSC amplitude normalized to first EPSC. Asterisk, $p<.05$. Error bars = SEM.

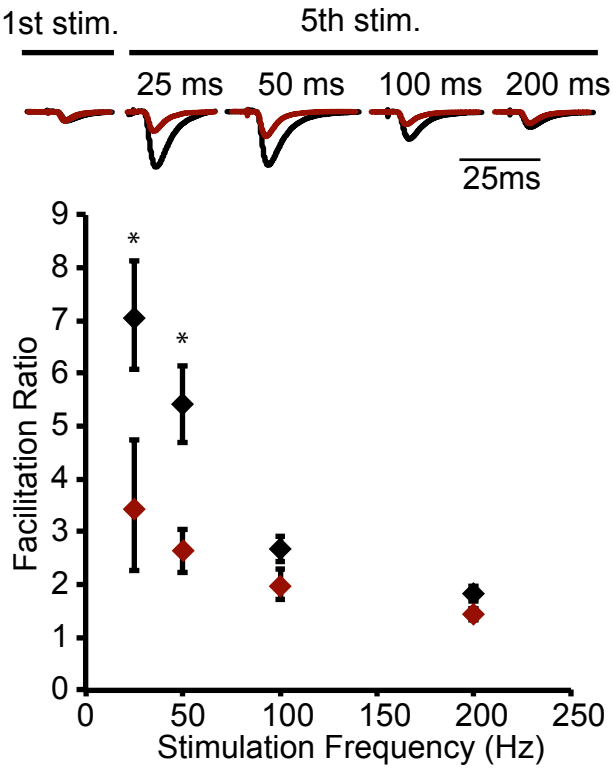

Figure 3.3 Frequency dependence of short-term facilitation.

Top, example cells comparing first to fifth EPSC at different interstimulus intervals. Bottom, population data for facilitation ratio, calculated as the amplitude ratio of the fifth EPSC to the first EPSC.

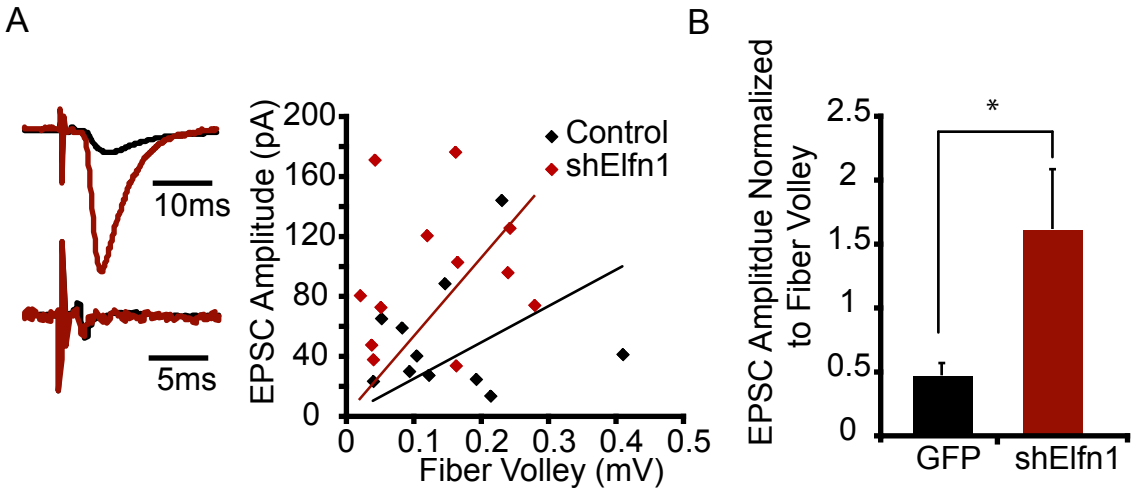

Figure 3.4 Elfn1 knockdown increases the evoked EPSC amplitude

A. Left, example traces from evoked EPSC amplitude, normalized to fiber volley recorded in the alveus adjacent to recording site. Right, scatter plot of EPSC amplitude as a function of the fiber volley recorded in the alveus.

B. Summary data showing average EPSC amplitude for control and knockdown neurons, normalized to fiber volley. Asterisk, $p<.05$ by t-test.

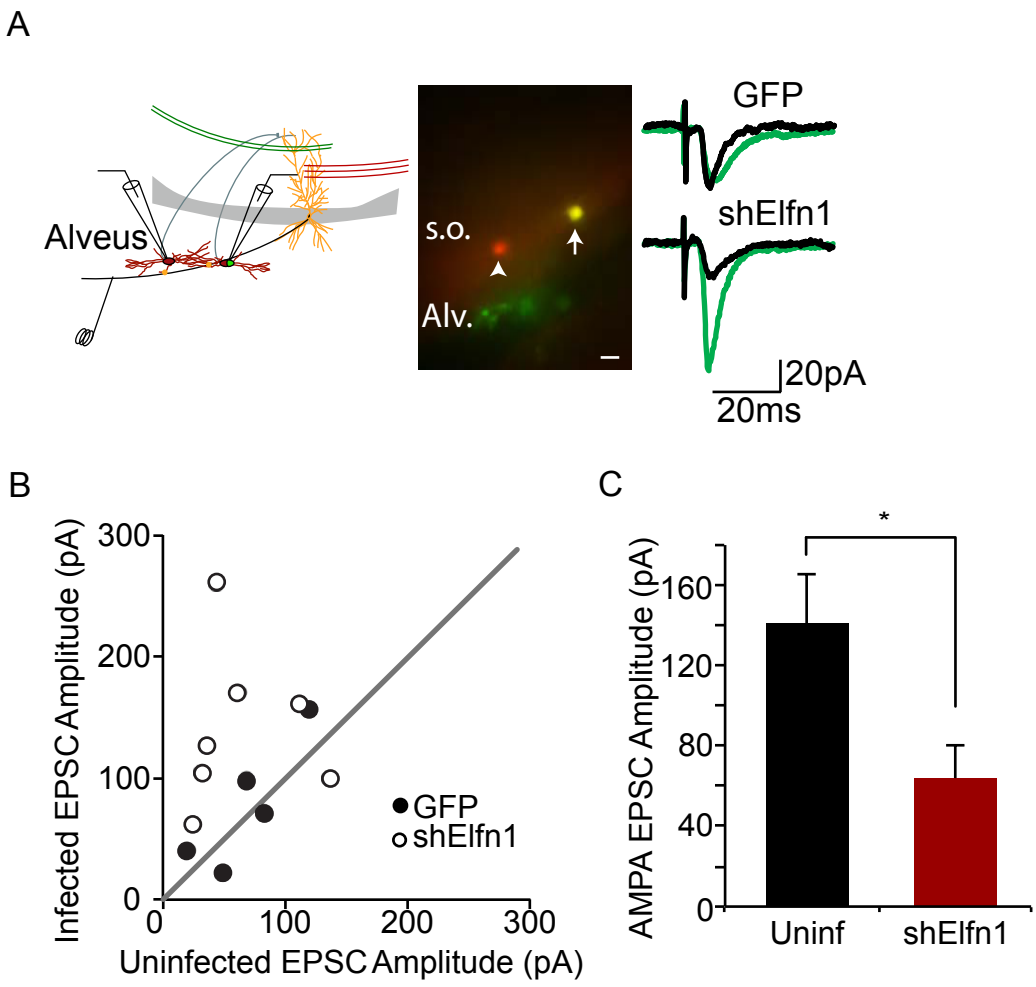

Figure 3.5 Elfn1 knockdown increases the evoked EPSC amplitude

A. Left, epifluorescent image of a simultaneuous recording from a pair of OLM inter-neurons, one infected and one uninfected. Right, sample average traces from the neurons shown at left.

B. Scatter plot of neighboring pairs. Each point represents one pair, where the unifected amplitude is plotted versus the infected amplitude. The gray line is unity.

C. Comparison of the mean AMPA EPSC amplitude for uninfected and shElfn1 infected neuorns in simultaneously recorded pairs.

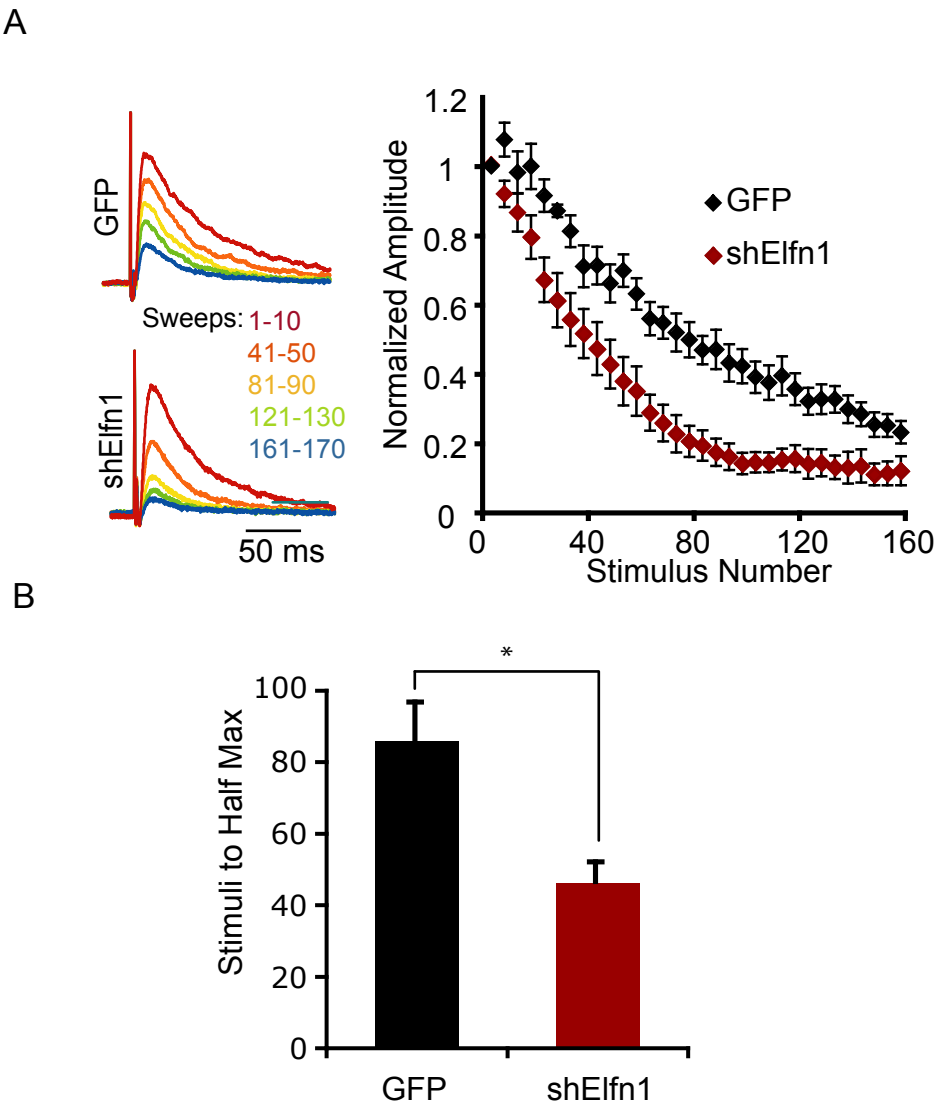

Figure 3.6 Elfn1 knockdown reduces facilitation by a presynaptic mechanism.

A. Left, example traces of NMDA EPSC at a holding potential of +40 mV in DNQX. Alveus is stimulated in the presence of 40 μM MK801. Right, average timecourse of the decrement of the NMDA current, binned every five stimuli and normalized to initial NMDA EPSC amplitude. GFP, n=7; shRNA, n=8.

B. Quantification of the number of stimuli at which the NMDA EPSC amplitude is reduced to half-max. $p<0.05$.

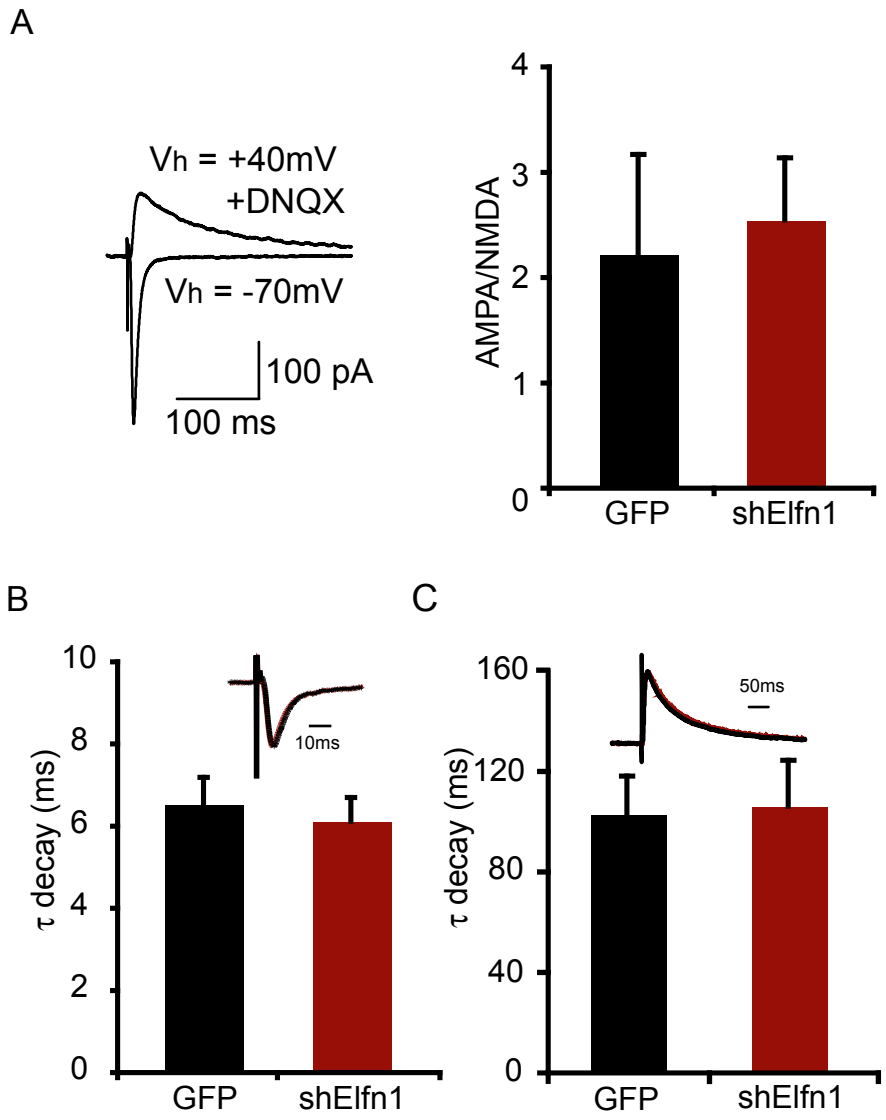

Figure 3.7 Postsynaptic properties of Elfn1 knockdown neurons.

A. Left, AMPA evoked EPSC from stimulation of the alveus, isolated at -70mV. NMDA mediated EPSC at +40mV, isolated by application of DNQX. Right, Quantification of the AMPA/NMDA ratio of CA1-Oriens interneuron synapses. GFP, n=7; shRNA, n=9.

B. Decay kinetics of AMPA EPSC. GFP, n=21; shRNA, n=15.

C. Decay kinetics of NMDA EPSC. n= 7 each condition.

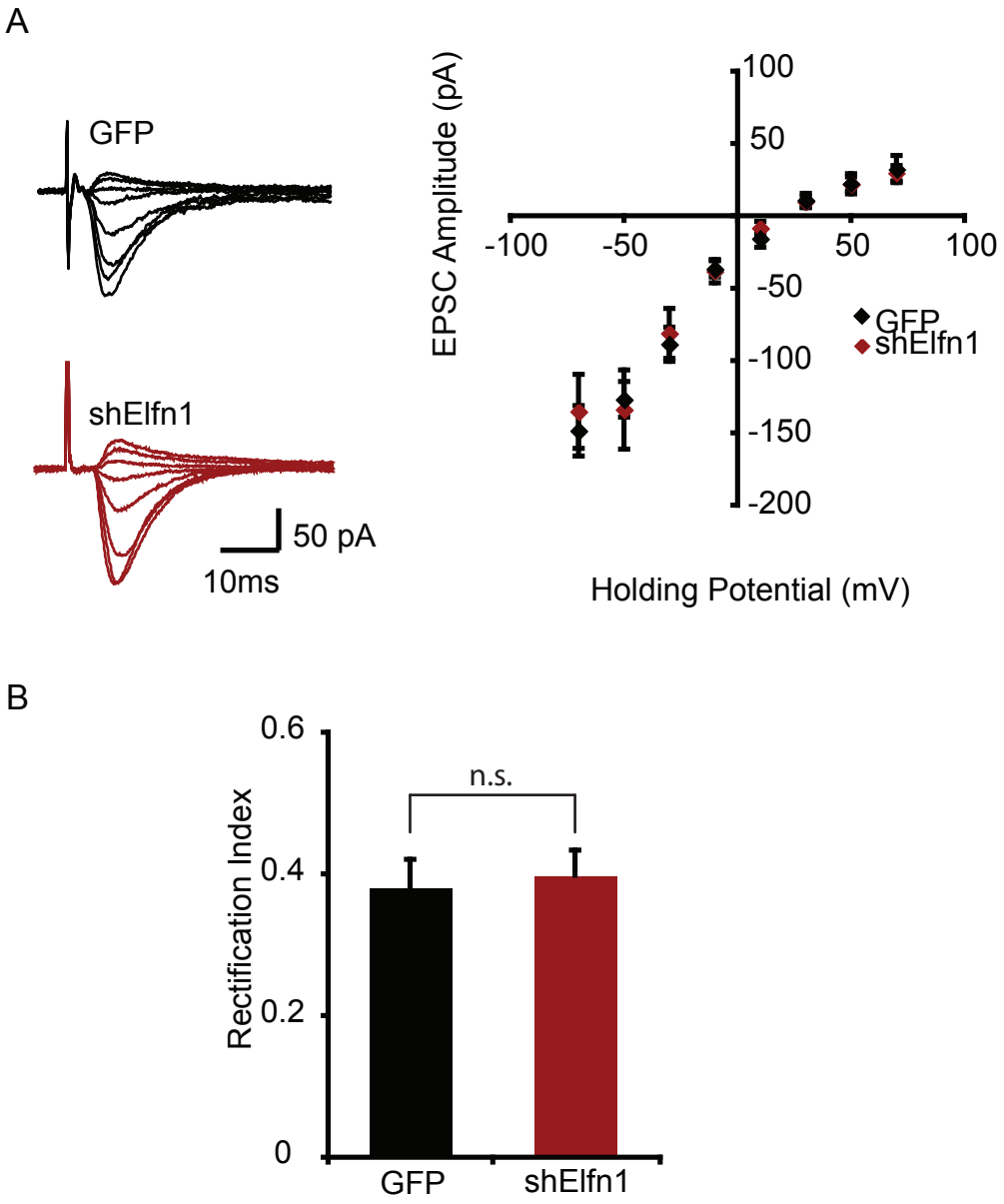

Figure 3.8 AMPA rectification is unchanged in Elfn1 knockdown neurons.

A. Examples traces and IV curve for AMPA mediate currents. Holding potential was varied between -70mV and +70 mV and the evoked response from alveus stimulation was recorded. GFP, n=6; shRNA, n=7.

B. Rectification index was calculated by the ratio of the slope of a line fit to the curve at 0mV to +70 mV to the slope of a line fit between -70 mV to 0mV.

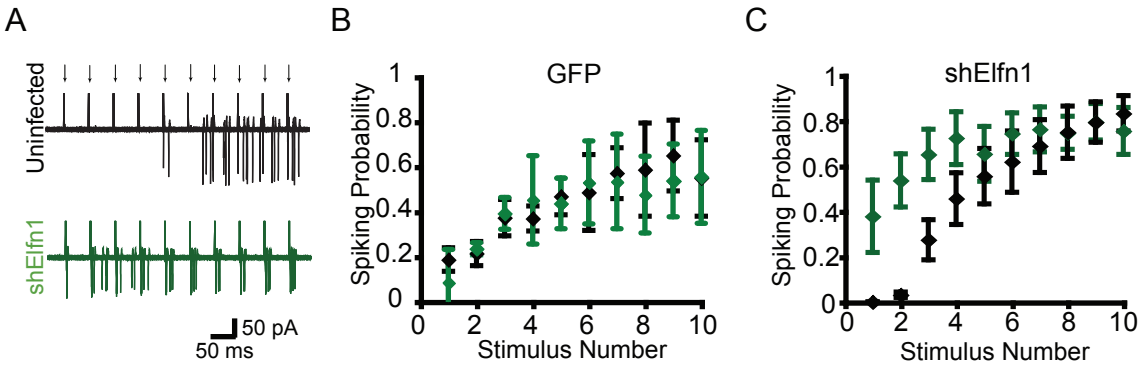

Figure 3.9 Elfn1 regulates the temporal dynamics of OLM interneuron recruitment

A. Simultaneuos recording in cell-attached configuration from neighboring uninfected and infected OLM cells. During recording, stimulus intensity was adjusted so that stimulus 5 ellicited a spike approximately 50% of the sweeps. Ten overlayed sweeps in response to 10 alvear stimulations at 20Hz, arrows indicate stimuli.

B. Average spiking probabilty to each stimulus as a function of stimulus number for pairs where the infected neuron is a GFP control.

C. Average spiking probabilty to each stimulus as a function of stimulus number for pairs where the infected neuron contains a shRNA to Elfn1.

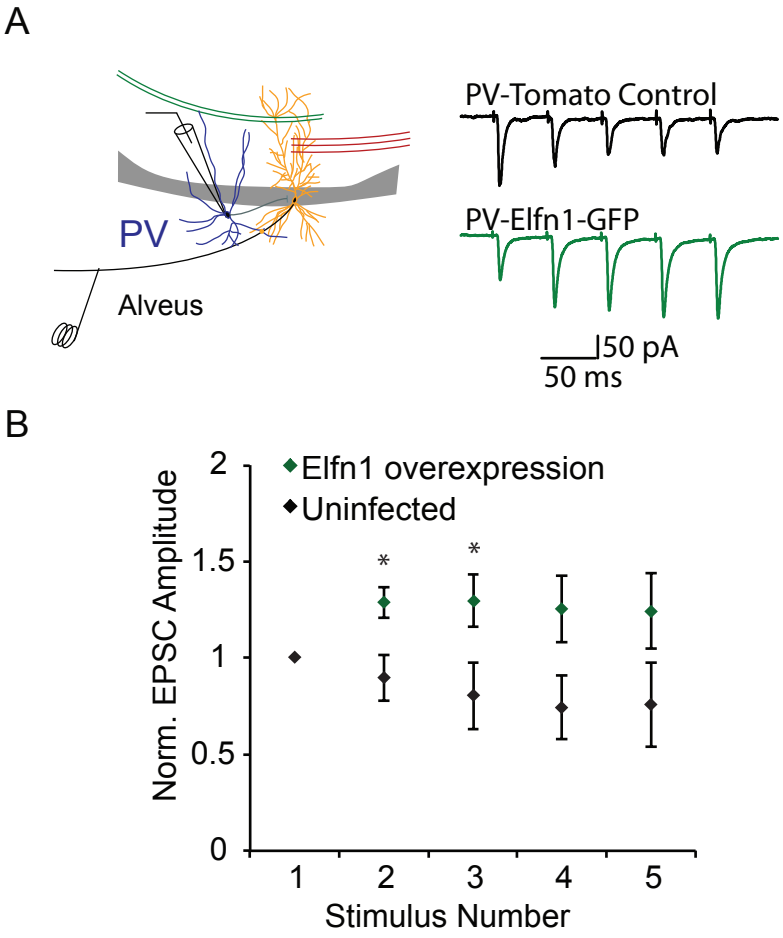

Figure 3.10 Elfn1 is sufficient to alter release probability at CA1 synapses.

A. Left, configuration for basket cell recording. A lentivirus overexpressing Elfn1-GFP is injected to P5 PV-IRES-Cre x LSL tdTomato mouse pups. Stratum pyramidale or statum oriens PV neurons in the infected area are targeted for recording. Right, Five stimuli are delivered to the alveus at 20Hz and the postsynaptic EPSC are measured.

B. Quantification of short-term plasticity in Elfn1 overexpressing PV cells. EPSC is normalized to first EPSC amplitude. Asterisk, $p<0.05$ by t-test.

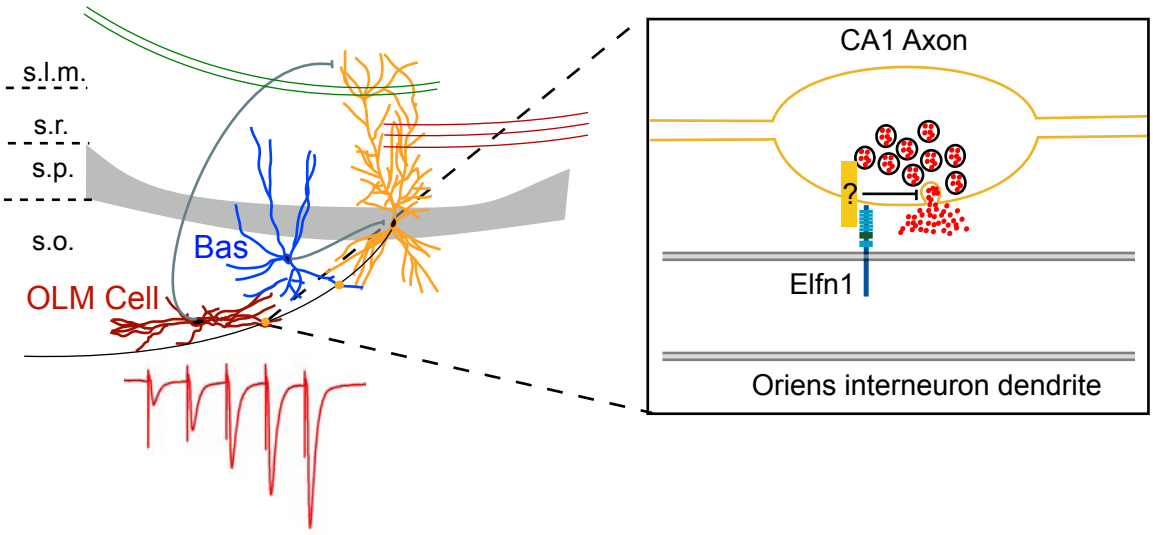

Figure 3.11 Model of Elfn1 function and CA1-Oriens interneuron synapses.

Elfn1 is present at the CA1 to OLM interneuron synapse at or near the post synaptic specialization. Elfn1 signals either indirectly through a postsynaptic cofactor, or directly through binding to an unknown presynaptic ligand. The effect of this interaction is to reduce probability of release, thereby increasing short-term facilitation.

CHAPTER 4: DISCUSSION OF THE ROLE OF ELFN1 IN SHORT-TERM PLASTICITY

4.1 ELFN1 REGULATES TARGET-CELL DEPENDENT SHORT-TERM FACILITATION

Regulating synaptic transmission is a fundamental aspect of neural circuit function and plasticity. Whether by altering calcium entry in the presynaptic terminal, properties of release machinery, number of docked vesicles, or postsynaptic receptor activation, subtle changes in synaptic transmission strongly influence information processing in the neural circuit. In the CA1 region of hippocampus, regulated control of short-term plasticity is a fundamental factor in the ability of neural circuits to route information between different outputs. CA1 pyramidal cell axons contact both basket cells and OLM interneurons, which represent fundamentally different outputs. Moreover, the presynaptic release properties of these two axon terminals depend on the postsynaptic target-cell type. It follows that a target-derived factor must exist to communicate with the presynaptic axon, initiating a retrograde signal denoting target-cell type. In this study, I use in situ hybridization and immunohistochemistry to show that the transmembrane molecule Elfn1, is specifically localized to this synapse. Furthermore, I find that Elfn1 is necessary for the hallmark property of this synapse, robust short-term facilitation. I verify that although knockdown of Elfn1 is postsynaptic, the effects of Elfn1 are of presynaptic origin. I propose that Elfn1 is the target-derived cue responsible for CA1 target cell specificity.

While initial studies with synaptic organizing molecules, such as the neurexin-neuroligin complex, showed robust and broad affects at either glutamatergic or GABAeric synapses (Scheiffele et al., 2000) (Chih et al., 2005), more recently, several synaptic organizing molecules have been shown to be restricted to particular classes of synapses. In the cerebellum, the Cbln1-GluRδ2 and Neurexin were shown to specifically regulate the parallel fiber-Purkinje cell synapse (Matsuda et al., 2010). The NGLs, a family of leucine-rich repeat (LRR) proteins, and their presynaptic partners the Netrin-Gs

are laminarly segregated between Schaffer collateral and temporal-ammonic synapses in the CA1 region of hippocampus (Nishimura-Akiyoshi et al., 2007). Although the specific localization of these proteins in intriguing, it is not clear if they correlate to specific physiological characteristics unique to their corresponding classes of synapses. Elfn1 is unique among cell adhesion molecules because it is only at fraction of synapses in the hippocampus, and it also regulates specific physiological properties at that synapse.

4.2 An Elfn1 transsynaptic complex

In light of the presynaptic locus of Elfn-1 mediated short-term facilitation, it will be interesting to investigate the mechanism of retrograde signaling. Elfn1 may act in *cis* with a cofactor that bridges the synapse, or it may bind directly to a presynaptic component to regulate release probability. The lack of any identified intracellular motifs, and the precedent for LRR domains to bind transsynaptically, as in the LRRTM2/Neurexin and Netrin-G/NGL binding pairs, would more strongly implicate a direct presynaptic partner. One candidate might be a neurexin isoform, which have been shown to be LRR binding proteins. Another candidate was recently identified in a large LRR binding screen in zebrafish. In this study, Elfn1 was identified to bind to the axonal protein Robo3 (Söllner and Wright, 2009), but I was unable to reproduce this finding in the mouse and no clear mechanism exists for how Robo3 could be influencing presynaptic release.

4.3 Mechanistic underpinnings of changes in release probability

Setting the synaptic bridging protein aside, there is still no presynaptic mechanism for Elfn1-dependent change in release probability. Other synaptic

organizing proteins have also been shown to influence various stages of vesicular release. Postsynaptic knockdown of classical cadherins changes short-term depression in cultured neurons via a deficit in vesicle recruitment to the active zone (Jungling, 2006). Another cell adhesion complex, Ephrin/EphB, can induce presynaptic long-term plasticity (Contractor, 2002). Furthermore, overexpression of PSD-95 in CA1 pyramidal cells can recruit a neuroligin/neurexin complex that functions to increase release probability (Futai et al., 2007). However, each of these instances describes proteins that are widely expressed and may set release probability at individual synapses, but not in a target-cell type dependent manner, like I see for Elfn1.

Although I have identified Elfn1 as a regulator of target-cell specific short-term facilitation, it is still unclear by what mechanism it changes presynaptic release. Owing to the interesting mechanisms of target-cell specificity, many studies have begun to unravel the presynaptic machinery involved in the expression of robust facilitation. A series of elegant experiments by Koester and Johnston showed that axons, in this case from cortical pyramidal neurons to two different targets, show larger calcium transients for the multipolar synapse (depressing) than the bitufted synapse (facilitating) (2005). In addition, analysis of the effects of different exogenous calcium buffers has concluded that facilitating synapses onto multipolar cells have a longer diffusional distance between calcium channels and calcium-dependent release machinery (Rozov et al., 2001).

Other studies have looked specifically at Schaffer collateral input to somatostatin interneurons in the stratum radiatum. Sun and Dobrunz and colleagues have found that the strong short-term facilitation at these synapses is a result of presynaptic kainate receptor activation (2006). They show that initial probability of release is lower at Schaffer collateral inputs onto Sst interneurons relative to pyramidal cells, in agreement with previous results (Rozov et al., 2001; Biro et al., 2005; Koester and Johnston, 2005).

However, during a train of stimuli to the Schaffer collaterals, glutamate release activates presynaptic kainate receptors and increases probability of release. Blocking kainate receptors attenuates facilitation at this synapse, suggesting that kainate receptor activation increases probability of release, either by direct calcium influx through calcium-permeable kainate receptors or indirectly by depolarizing the presynaptic terminal (Sun and Dobrunz, 2006). It would be interesting to see if Elfn1 regulation of short-term facilitation rests on changes in basal release probability, activation of presynaptic kainate receptors, or both.

4.4 Convergent mechanisms for regulation of release probability

It should be noted that while there is a striking decrease in the short-term facilitation at CA1-OLM synapses, it is not abolished. This may reflect an incomplete knockdown of Elfn1 or the presence of other factors in determining release probability. Preliminary data has shown that overexpression of Elfn1 can change facilitation in cells that lack endogenous Elfn1, suggesting that Elfn1 is sufficient to change release probability. However, it may be one of several molecules that contribute to release, albeit a very influential molecule. It is possible that the relative amounts of other of the more ubiquitously expressed molecules, such as cadherins or neurexin/neuroligin complexes, may also be regulated at these synapses to further affect release probability. On way to address this question is with genetic deletion of Elfn1.

4.5 Generalizing the role of Elfn1 in short-term plasticity

Interestingly, mRNA expression data would suggest that Elfn1 is coexpressed with other populations of somatostatin cells in the brain that have similar characteristics. We find that E

Elfn1 colocalizes with Sst cells in the cortex as well. Somatostatin cells in the cortex include Martinotti cells, which are the cortical equivalent of OLM cells in structure and function. Like OLM cells, they also have facilitating inputs from pyramidal cells and similarly provide inhibition to the distal dendrites (Wang, 2004). In the dentate gyrus, the HIPP cell is the OLM interneuron counterpart. In like kind, they provide recurrent inhibition on the distal dendrites of granule cells (Han et al., 1993). Elfn1 colocalizes with both of these cell types, so it will be interesting to determine if the function of Elfn1 can be generalized. If this is true, Elfn1 can be more broadly defined as a target-derived factor whose presence instructs the formation of a facilitating synapse.

4.6 Functional role of facilitating synapses onto OLM cells

Neuronal circuits use the timing and frequency of action potentials to encode features of sensory stimuli. CA1 axons distribute output to two different interneuron populations that separately encode each parameter. The timing of CA1 activity is captured in the basket cells, as their strong but rapidly depressing response reliably follows the onset of CA1 activity. The frequency of CA1 activity is encoded by OLM interneurons, whose facilitating synapses ensure that they are only recruited after repetitive firing in CA1. The arrangement and function of these cell types is also important for circuit-wide activity in the hippocampus. Hippocampal theta rhythms have been linked to several behavioral states, including active exploration (Vanderwolf, 1969) and memory formation or retrieval (Larson et al., 1986; Buzsaki, 1989). It has been demonstrated *in vivo* that interneurons are phase-locked to theta rhythms in a cell-type specific manner (Klausberger et al., 2003). Computational modeling has shown that theta rhythms can be generated using a circuit consisting of pyramidal cells, basket and OLM interneurons (Rotstein et al., 2005; Orban et al., 2006). The strong

afterhyperpolarization in OLM cells as well as a more quickly depressing synapse onto the basket cell were shown to be key elements to locking in a theta rhythm *in silico*.

Input arriving to OLM cells is routed to the distal dendrites of CA1 pyramidal cells. It would be interesting to explore any downstream consequences of Elfn1 manipulations to these targets of OLM cells. The distal dendrites of CA1 pyramidal cells also receive synapses from entorhinal cortex (temporoammonic pathway) and the timing of inhibition arriving from CA1 via OLM interneurons and excitation from the perforant path may be important for dendritic processing in CA1 interneurons. Activation of Schaffer collateral inputs one-half theta cycle prior to temporoammonic pathways results in a supralinear summation of the two inputs, but only in the absence oriens interneuron activation, though this includes a combination of Sst and PV interneurons (Ang et al., 2005). Ang and colleagues have proposed that feedback inhibition may serve to switch the CA1 neurons between two distinct functional states (Ang et al., 2005). In one state, strong Schaffer collateral input brings CA1 neurons above threshold to spike, thereby engaging feedback inhibition via the oriens interneurons, which in turn suppress interfering temporoammonic input. In contrast, during theta rhythms that occur in exploratory behavior, CA1 place cells show increases in activity and interneurons show activity suppression (Nitz and McNaughton, 2004). In the lack of strong feedback inhibition, Schaffer collateral and temporoammonic pathways interact cooperatively, which may provide a mechanism to select for match/mismatch activity in novelty detection (Ang et al., 2005). The role of synapse-specific short-term plasticity in maintaining these segregated networks is unclear. However, it is likely that altering the precise temporal recruitment of feedback inhibition by modulating short-term plasticity will affect circuit dynamics.

4.7 ELFN1 IS A TARGET-CELL DERIVED CUE

The diverse morphological and physiological characteristics of synapses are well described, however, the organizing principles of this synaptic diversity have still not been clearly defined. The unique role of Elfn1 at a specific set of synapses described here, as well as other recent data on synaptic organizing molecules has begun to shed light on their various physiological roles and synapse-specific localization. More importantly, Elfn1 provides a mechanism for the fundamental phenomenon that an individual axon can distinguish between two different postsynaptic targets and adjust presynaptic properties accordingly, a fact that is essential for the function of neural circuits.

CHAPTER 5: ROLE OF MECP2 IN ACTIVITY-DEPENDENT HOMEOSTATIC PLASTICITY

5.1 INTRODUCTION

Synaptic scaling is a form of plasticity in which neuronal activity drives cell-wide changes in synaptic strength (Turrigiano et al., 1998; Davis, 2006; Turrigiano, 2007; Turrigiano, 2008). In general, an increase in neuronal activity leads to a decrease in quantal amplitude, and a decrease in activity leads to an increase in amplitude. It is believed that such homeostatic regulation of synaptic strength is important for maintaining action potential firing rates in a range suitable for information processing (Davis, 2006; Turrigiano, 2007; Turrigiano, 2008).

There is considerable evidence that changes in synaptic strength associated with synaptic scaling are mediated by changes in the levels of AMPA receptors (O'Brien et al., 1998; Turrigiano et al., 1998; Shepherd et al., 2006; Gainey et al., 2009). Most AMPA receptors in the brain consist of GluR1/GluR2 or GluR2/GluR3 heterodimers and scaling up of synaptic currents following silencing of neurons is associated with an increase in synaptic GluR1 and GluR2 receptors (O'Brien et al., 1998; Thiagarajan et al., 2005; Turrigiano, 2008; Gainey et al., 2009). More recently, it has also been shown that GluR2 is required for photostimulation-dependent homeostatic decreases in synaptic strength (Goold and Nicoll, 2011).

The molecular mechanisms by which chronic changes in neuronal activity lead to scaling of synaptic currents are not well understood. In contrast to rapid forms of synapse modification, such as long-term potentiation (LTP) and long-term depression (LTD), changes in synaptic strength associated with synaptic scaling are detected several hours to days after a change in network activity and require transcription (Ibata et al., 2008). Studies investigating synaptic scaling have implicated BDNF, TNFα, β3 integrin, MHC I, CaMKIV, and Arc in scaling up of synaptic currents following silencing of neurons (Turrigiano, 2008). The mechanisms underlying scaling down of synaptic

currents in response to elevated activity have not been as extensively studied, but a recent study suggests a role for polo-like kinase 2 (Plk2) in this process (Seeburg et al., 2008). Plk2 is an activity-induced gene, and appears to act by regulating the degradation of SPAR, a protein implicated in regulating spine morphology and synaptic function.

In light of the observation that synaptic scaling is associated with a change in levels of AMPA receptors, we decided to explore activity-dependent mechanisms that might regulate overall AMPA receptor levels in response to elevated activity. Our observations reveal a novel pathway by which activity can regulate AMPA receptor levels, thereby controlling synaptic strength. Here we report that the Rett syndrome protein MeCP2 plays a critical role in mediating activity-dependent changes in GluR2 levels and is required for synaptic scaling.

5.2 METHODS

Plasmids Lentiviral vectors were from Dr. I. Verma's lab at the Salk Institute. The LEMPRA strategy for lentiviral shRNA delivery and rescue that we used is described in (Zhou et al., 2006). We generated an HA-MeCP2 shRNA resistant construct for MeCP2 rescue expression. Short hairpin sequence and rescue shRNA resistant construct sequences are described in (Zhou et al., 2006). The hUbiquitin promoter was taken from FUGW construct (Addgene).

Molecular Biology reagents: Molecular biology reagents, competent cells, real-time PCR mix and reverse transcription kits were from Biopioneer. Inc. (San Diego, CA).

Antibodies Antibodies used were the following: MeCP2 rabbit polyclonal antibody

(Abcam, Upstate, Qiu Lab); HDAC1, mSin3A, ERK1 and control rabbit IgG (Santa Cruz Biotechnology); GluR2 MAB397 (Chemicon).

Mice *mecp2* conditional knockout mice made in Rudolf Jaenisch's lab were used for dissociated neuronal cultures (Chen et al., 2001). *mecp2* knockout mice generated in Adrian Bird's lab were used for hippocampal slice culture (Guy et al., 2001).

Cell culture For biochemical experiments, E18 rat cortical cells were cultured in 12-well plates as previously described (Song and Ghosh, 2004). Cultures were stimulated at 14 DIV with 50μM bicuculline (in DMSO) to increase synaptic activity. The cultures were pretreated with 10μM nifedipine for 1 hour to selectively drive NMDA receptor-dependent calcium influx. For activity-dependent changes in gene expression, E18 cortical cultures at 16 DIV were stimulated for 6 hours with bicuculline and changes in gene expression were assessed using an Affimetrix rat 230A microarray chip. For electrophysiology experiments, P0-1 rat hippocampal cells were cultured on thermanox coverslips (Nunc) in 12 well plates, electroporated at plating or infected with Lentivirus at 7/8DIV with control shRNA or MeCP2 shRNA, stimulated at 12DIV with 50μM bicuculline (in DMSO), and recorded at 14DIV.

Chromatin immunoprecipitation ChIP assays were performed as originally described with minor modifications (Song and Ghosh, 2004). Primers: rat GluR2 F: GCCCAGAGCTCCGACTAAAG , R: GGCAGTCTCGGGCGCGCGTG, rat GluR1 F: GAGGAGAGAGGCTGCCTGCT, R: CCCTCCCCTCCCTTCGATTC, mouse MeCP2 F: cgcgcgcaaccgatgccgggacc, MeCP2 R: ccgcctcttttccctgcctaaaca .

Real time quantitative RT-PCR Total RNA was collected from cell lysates for reverse

transcription. First strand cDNA synthesis kit from BioPioneer was used for cDNA synthesis. Primers for rat GluR2 cDNA is F: GAAGCCTTGTGACACCATGA , R: AGCCTTGCCTTGCTCCTCAT. Mouse and rat MeCP2 cDNA is F: ATGGTAGCTGGGATGTTAGGG , R: TGAGCTTTCTGATGTTTCTGCTT . For real time PCR experiments, SYBR Green PCR master mix from Applied Biotechnology and 2XqPCR master mix from BioPioneerinc.com were used. An ABI 7000 Q-PCR machine was used to perform the experiments. Data sets are from at least two independent experiments, each of which had triplicate samples. Paired t tests were performed using GraphPad InStat version 3.0a for Macintosh, GraphPad Software (San Diego, CA).

Electrophysiology Electrophysiological recordings were performed on neurons from hippocampal cell cultures (P0-1+14 DIV), perfused at room temperature in a bicarbonate buffered recording solution containing the following (in mM): 124 NaCl, 5 KCl, 26 $NaHCO_3$, 1.25 NaH_2PO_4, 1.5 $MgCl_2$, 2 $CaCl_2$, and 10 glucose and bubbled constantly with 95% O_2/5% CO_2. Voltage-clamp recordings were made using glass microelectrodes (borosilicate glass, 1.5 mm outer diameter and 1.16 mm inner diameter; Warner Instruments) pulled on a micropipette puller (Flaming-Brown P-80/PC; Sutter Instruments, Novato, CA) and filled with a cesium substituted intracellular solution containing (in mM) 10 CsCl, 105 $CsMeSO_3$, 8 NaCl, 0.5 ATP, 0.3 GTP, 10 HEPES, 2 $MgCl_2$, and 1 EGTA, pH 7.3. Drug concentrations were (in μM): 0.5 TTX, 50 D-APV, 20 Gabazine. Pipette resistances ranged from 4 to 6 MΩ. Series resistances ranged from ~8 to 20 MΩ and were monitored for consistency during recording using a -5mV test pulse. Whole-cell voltage-clamp recordings at -70 mV were made using a Multiclamp 700B amplifier (Molecular Devices). Current signals were filtered at 2 kHz and digitized at 10 kHz with a Digidata 1322A. Gabazine (SR 95531 hydrobromide) and D-APV were

added at the time of recording and were acquired from Tocris Chemicals (Ellisville, MO). TTX was acquired from Sigma-Aldrich. mEPSCs were identified and isolated using ClampFit software. Using a control culture, a template was created from a composite average of manually identified mEPSCs and was used with a high threshold for deviation to ensure all events in subsequent recordings were captured. These events were then manually inspected to discard any non-EPSC traces.

5.3 RESULTS

Synaptic Scaling is accompanied by down-regulation of GluR2 mRNA and protein.

We carried out whole cell voltage-clamp recordings from postnatal day 0-1 (P0-1) hippocampal cultures to examine the effect of a bicuculline-induced increase in neuronal activity on scaling of synaptic currents. As shown in Figure 5.1, spontaneous mEPSCs are readily detected in hippocampal cultures at 14 days in vitro (DIV). As previously described (Turrigiano et al., 1998), 48 hr bicuculline treatment led to a decrease of ~20% in average mEPSC amplitudes (Fig. 5.1). Intrinsic membrane properties and recording parameters were monitored, and control and bicuculline treated neurons showed no difference in membrane capacitance, input resistance, series resistance, and baseline noise.

The reduction in mEPSC amplitudes is consistent with the report that bicuculline treatment leads to a reduction in postsynaptic response to glutamate (Turrigiano et al., 1998). To determine if this is accompanied by a reduction in the abundance of AMPA receptors, we carried out real-time PCR and Western Blot analysis to determine if bicuculline treatment affects the expression of AMPA receptor subunits. Treatment of cultures with bicuculline for 6 hours led to a decrease in GluR2 mRNA levels, but not

GluR1 mRNA levels (Figure 5.2), indicating that elevated activity leads to a decrease in GluR2 gene expression (O'Brien et al., 1998; Grooms et al., 2006). GluR2 protein levels in both dissociated and slice cultures were also significantly reduced following bicuculline treatment (Figure 5.2). The decrease in GluR2 mRNA levels was blocked by the NMDA receptor antagonist, APV. The inclusion of NMDA did the grossly affect the stimulation intensity, since in control experiments the synaptic activation in response to bicuculline, as measured by charge transfer, did not differ between control and APV treated cultures (data not shown). These observations suggest that activity-dependent scaling of synaptic current involves NMDA receptor-dependent down-regulation of GluR2 expression.

MeCP2 is recruited to the GluR2 promoter following stimulation.

To explore the possibility that the reduction in GluR2 expression in response to elevated activity is mediated by a transcriptional repressor, we carried out a microarray screen for repressor genes that are induced by bicuculline stimulation (data not shown). One gene that was strongly induced by bicuculline stimulation was the methyl CpG-binding protein MeCP2 (Figure 5.3). MeCP2 is a transcriptional repressor that has been extensively studied in the context of Rett syndrome, in which the gene is mutated (Meehan et al., 1992; Amir et al., 1999; Chahrour and Zoghbi, 2007). Given the potential clinical significance of a role for MeCP2 in regulating the response to a global increase in cellular activity, we were motivated to examine whether MeCP2 was involved in regulating GluR2 levels. In support of such a possibility, the GluR2 promoter has been reported to be methylated (Myers et al., 1998), which could facilitate recruitment of MeCP2 (Skene et al., 2010). To determine if MeCP2 was associated with the GluR2 promoter, we carried out chromatin immunoprecipitation (ChIP) experiments on lysates

from cortical cultures. Analysis by quantitative PCR indicated that MeCP2 is bound to the GluR2 promoter (Figure 5.3). Additional ChIP experiments revealed that the transcriptional co-repressors HDAC1 and mSin3A also bind to the GluR2 promoter, suggesting that GluR2 expression may be regulated by a repressor complex (Figure 5.3). To determine if occupancy of the GluR2 promoter by MeCP2 was regulated by activity, we carried out ChIP experiments from control and bicuculline stimulated cultures and found that bicuculline leads to an increase in the binding of MeCP2 to the GluR2 promoter (Figure 5.3).

We next wanted to determine whether MeCP2 was required for activity-dependent down-regulation of GluR2 expression. For these experiments we generated a short hairpin RNA against MeCP2 and cloned it into a lentiviral expression vector. As shown in Figure 5.4, this shRNA was very effective in down-regulating MeCP2 expression in hippocampal cultures. To test the role of MeCP2 in the bicuculline-induced decrease in GluR2 expression, we examined GluR2 levels in control and MeCP2 shRNA-expressing cultures. As described above for uninfected cultures, bicuculline stimulation of cultures infected with a control shRNA led to a decrease in GluR2 expression (Figure 5.4). This decrease was blocked in cultures expressing the MeCP2 shRNA lentivirus, suggesting that MeCP2 was required for activity-dependent down-regulation of MeCP2 (Figure 5.4). In support of the specificity of shRNA experiment, we found that expression of an shRNA-resistant same-sense mutant of MeCP2 rescued the activity-dependent down-regulation of GluR2 (Figure 5.4).

To determine if genetic deletion of MeCP2 also affected activity-dependent down-regulation of GluR2 expression, we cultured hippocampal slices from wild type and *mecp2* null mice and compared the effects of bicuculline stimulation on GluR2 expression. As in the case of rat hippocampal cultures, bicuculline treatment led to a

decrease in GluR2 protein levels in wild type mouse cultures (Figure 5.4). In contrast, bicuculline treatment did not lead to a down-regulation of GluR2 levels in *mecp2* null cultures, indicating that endogenous MeCP2 is required for activity-dependent down-regulation of GluR2 levels (Figure 5.4).

MeCP2 is required for synaptic scaling in response to elevated network activity.

To determine whether MeCP2-dependent regulation of GluR2 was required for activity-dependent synaptic scaling we measured mEPSC amplitude in hippocampal cultures in which MeCP2 levels were down-regulated by shRNA expression or gene deletion. In the first set of experiments, we infected hippocampal cultures with lentiviruses encoding GFP or GFP with shRNA targeting MeCP2 at 5 DIV, stimulated with bicuculline at 12 DIV, and recorded from GFP positive neurons at 14 DIV. GFP-infected neurons showed a decrease in mEPSC amplitude following bicuculline treatment (Figure 5.5). Strikingly, this bicuculline-induced scaling of mEPSC amplitudes was absent in neurons expressing MeCP2 shRNA (Figure 5.5). This was not due to a failure of synaptic activation in MeCP2 shRNA expressing cells, as the bicuculline-induced increase in charge transfer was similar in control and MeCP2 shRNA expressing cells. Expression of an shRNA-insensitive rescue construct fully restored bicuculline-induced scaling, indicating that activity-dependent scaling down of synaptic currents requires MeCP2 (Figure 5.5)

In a complementary set of experiments we asked whether genetic deletion of MeCP2 would also prevent synaptic scaling. For these experiments, we cultured neurons from conditional *Mecp2* mutant mice at P0 (Chen et al., 2001). The cultures were electroporatated with either GFP alone or GFP and a Cre-expression construct at the time of plating, and the cultures were treated with bicuculline at 13 DIV for 48 hours.

In contrast to control neurons, which showed bicuculline-induced scaling of mEPSC amplitudes similar to that seen in rat hippocampal cultures, there was no synaptic scaling in Cre-expressing neurons (Figure 5.6). In contrast to the shRNA experiments in rat cultures, there was also a decrease in mEPSC amplitudes under control conditions in the mouse cultures (Figure 5.6). This may reflect a more complete loss of MeCP2 function in the mouse cultures where MeCP2 is genetically deleted. The data from the knockdown and conditional deletion of MeCP2 indicate that endogenous MeCP2 is required for bicuculline-induced synaptic scaling.

5.4 CONCLUSIONS

The observations reported here reveal a role for MeCP2 in activity-dependent scaling of synaptic inputs. We find that increased activity leads to induction of MeCP2 expression. MeCP2 in turn binds to the GluR2 promoter and recruits a repressor complex to inhibit GluR2 expression. Loss of MeCP2 by shRNA expression or genetic deletion blocks activity-dependent decrease in GluR2 expression and synaptic scaling. Based on these findings, we suggest that the MeCP2-dependent decrease in synaptic AMPA receptors leads to the observed scaling of synaptic strength. MeCP2 has many transcriptional targets and global changes in activity lead to structural reorganization in addition to scaling of synaptic currents. MeCP2 provides a mechanism by which activity can trigger a change in the expression of several genes and produce a variety of different cellular modifications.

Acknowledgments

The experiments described here in Chapter 5 are the product of collaboration with Dr. Zilong Qiu, who performed the biochemistry and molecular biology experiments. I performed the electrophysiolgical analyses. The resulting manuscript is in press: Qiu Z, Sylwestrak EL, Leiberman DN, Zhang Y, Liu X, and Ghosh A, “The Rett Syndrome Protein MeCP2 Regulates Synaptic Scaling”.

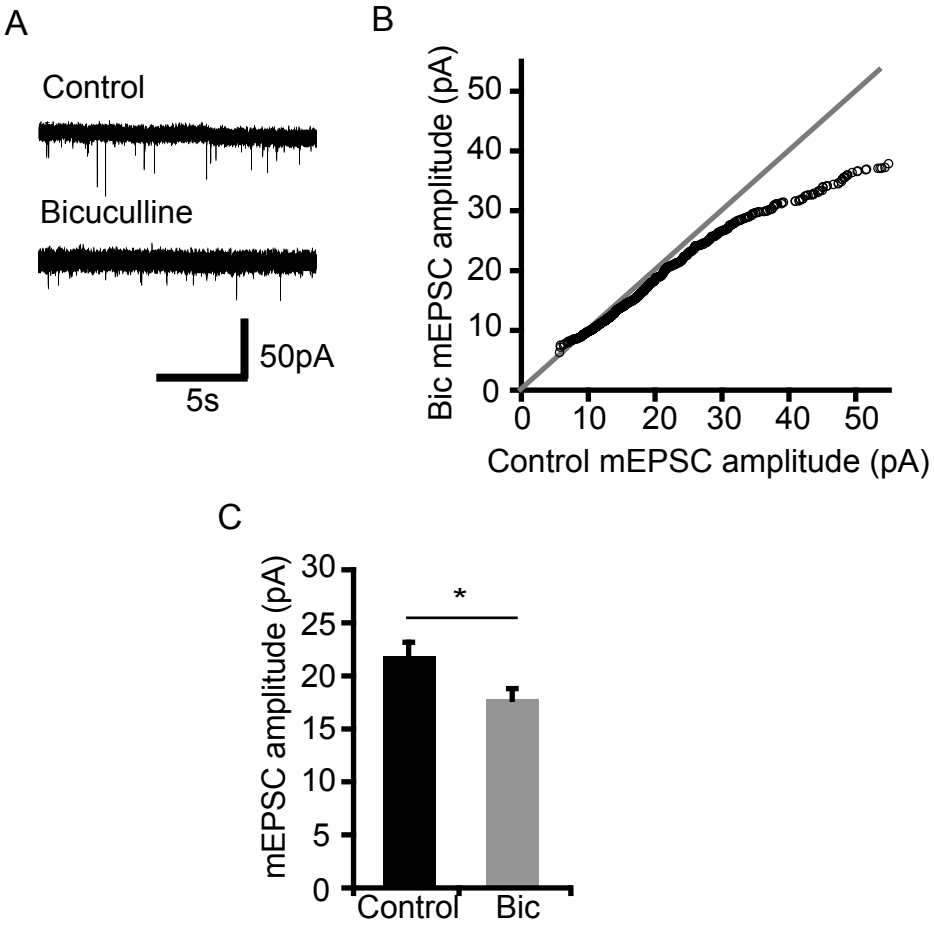

Figure 5.1 Bicuculline stimulation induces synaptic scaling

A. Representative 15 sec mEPSC recordings from hippocampal neurons at P0+14DIV grown under control conditions or treated with 50μM bicuculline for 48 hrs prior to recording.

B. Amplitudes of mEPSC from control cultures or cultures treated with 50 μM bicuculline for 48 hrs prior to recording. mEPSCs for each treatment were sorted and the resulting distributions were plotted against each other. n=24 (control), 23 (bicuculline) cells. For clarity, only mEPSCs under 55pA are shown.

C. Quantification of average mEPSC amplitude (mean ± SEM). n=24 (control), 23 (bicuculline). $p < 0.05$, t-test.

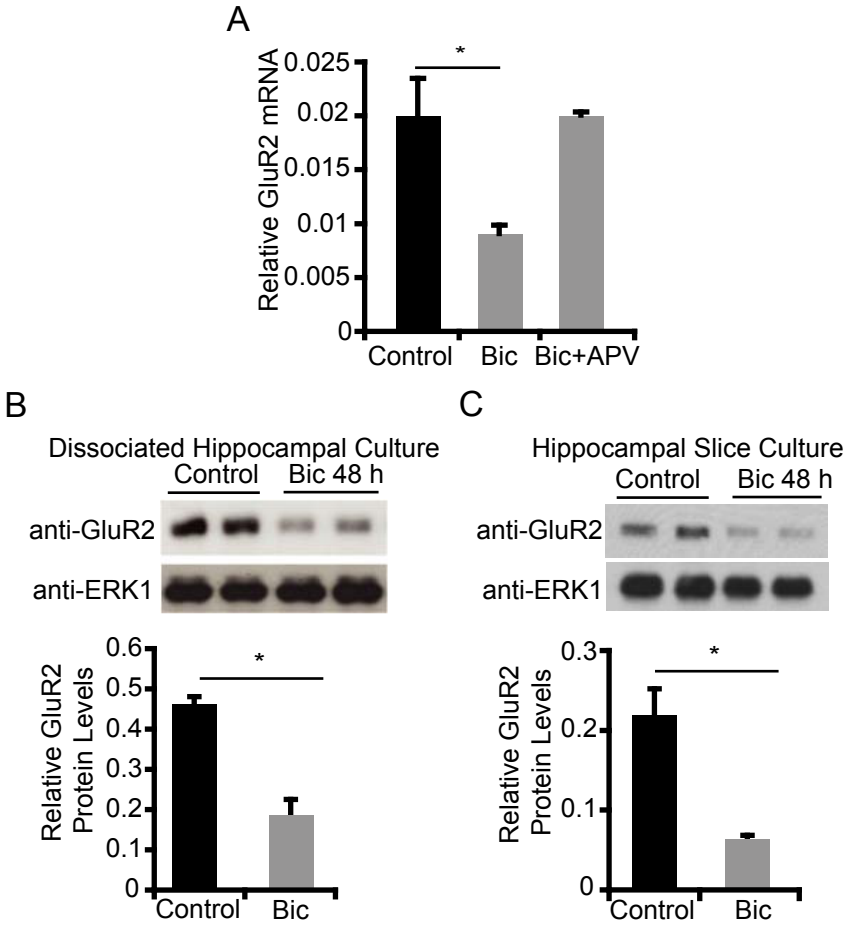

Figure 5.2 Synaptic scaling is accompanied by down-regulation aof GluR2 mRNA and protein

A. Assessment of GluR2 mRNA levels in rat E18 cortical cultures at 18 DIV, grown under control conditions, or treated with bicuculline for 6 hrs prior to cell lysis. Cultures were pretreated with APV for 1 hr where indicated. Neurons were lysed for collecting total RNA, and reverse-transcribed for real-time PCR analysis with GluR2 specific primers.

B. Assessment of GluR2 protein levels in dissociated neuronal culture after bicuculline treatment. Rat P0 hippocampal neurons were cultured for 14DIV and stimulated with bicuculline for 48 hours. Neurons were lysed, analyzed by SDS-PAGE, and blotted with antibody indicated.

C. Assessment of GluR2 protein levels in hippocampal slice culture after bicuculline treatment. Hippocampal slices from rat P7 pups were cultured for 3DIV and stimulated with bicuculline for 48 hours. Neurons were lysed, analyzed by SDS-PAGE, and blotted with antibody indicated.

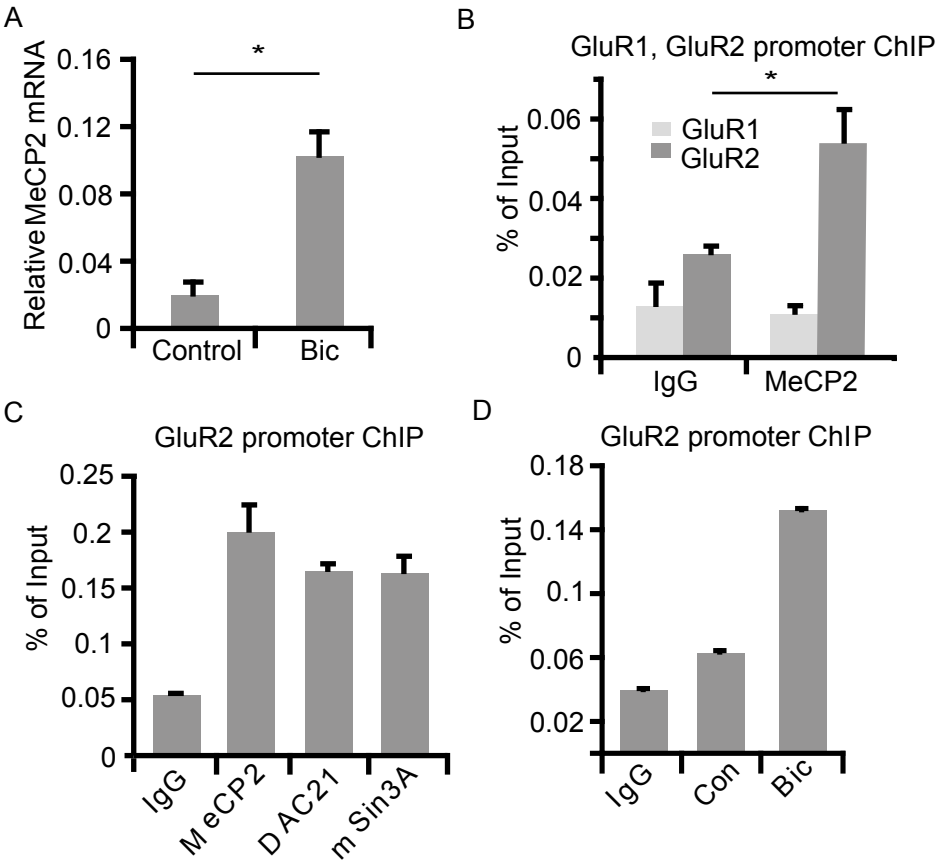

Figure 5.3 MeCP2 is required for activity-dependent down-regulation of GluR2 expression

A. Assessment of MeCP2 mRNA after bicuculline stimulation. Rat E18 cortical neurons were cultured for 16DIV and stimulated with bicuculline for 6 hours. Neurons were lysed for collecting total RNA and reverse-transcribed for real-time PCR analysis with MeCP2 specific primers.

B. MeCP2 chromatin immunoprecipitation from rat cortical cultures at E18+7 DIV. After immunoprecipitation with anti-MeCP2 antibody, PCR reactions with endogenous GluR1 and GluR2 promoter primers were used to amplify promoter-specific segments. Real time quantitative PCR was normalized to input.

C. MeCP2, HDAC1 and mSin3A chromatin immunoprecipitation from rat cortical neurons at E18+7 DIV under basal conditions. After immunoprecipitation with anti-MeCP2, anti-HDAC1 and anti-mSin3a antibody, PCR reactions with endogenous GluR2 promoter primers were used to amplify GluR2 promoter-specific segments. Real time quantitative PCR was normalized to input.

D. Relative binding of MeCP2 to the GluR2 promoter in unstimulated and bicuculline-stimulated neurons examined using chromatin immunoprecipitation.

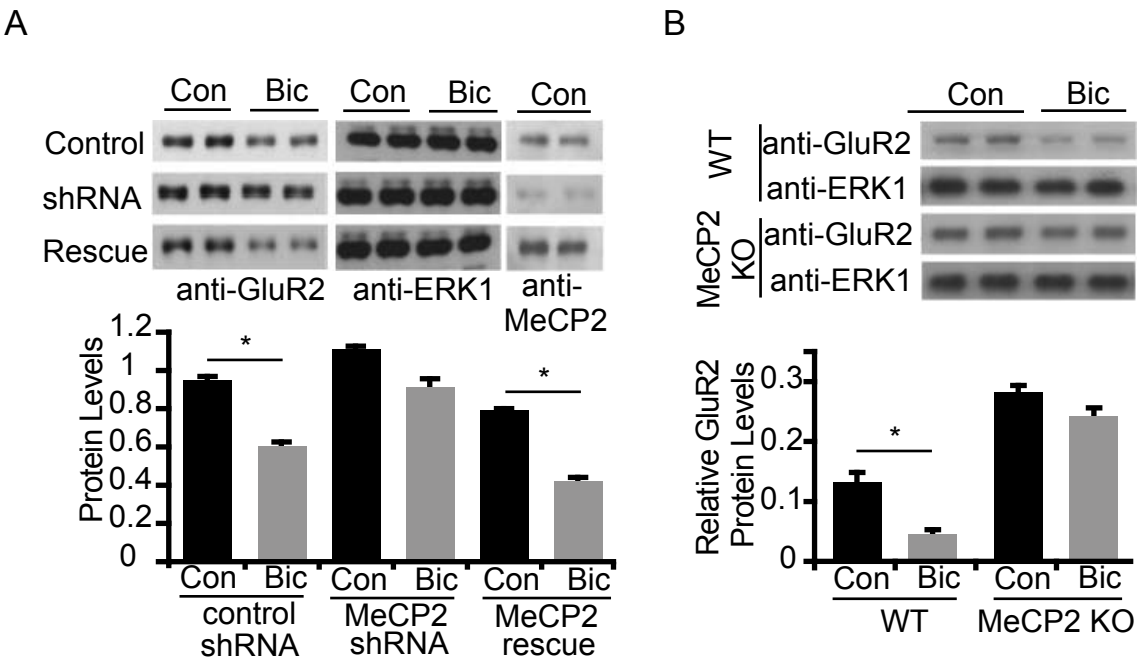

Figure 5.4 MeCP2 is necessary for bicuculline induced changes in GluR2 expression

A. Assessment of changes in GluR2 expression following bicuculline stimulation, with and without MeCP2. Rat P0/P1 hippocampal neurons were cultured for 8DIV and infected with lentivirus containing control shRNA, MeCP2 shRNA and MeCP2 shRNA with shRNA resistant MeCP2, respectively. Cultures were stimulated with bicuculline for 48 hours where indicated, and lysed for Western blot analysis with specified antibodies. Asterisk indicates $P<0.05$ using t test.

B. Assessment of changes in GluR2 protein levels following bicuculline stimulation in wild type and MeCP2 knockout neurons. P7 hippocampal slices were prepared from wild type and MeCP2 knockout mouse and cultured for 3 days. After stimulated by bicuculline for 48 hours, neurons were lysed for Western blot analysis with specified antibodies indicated.

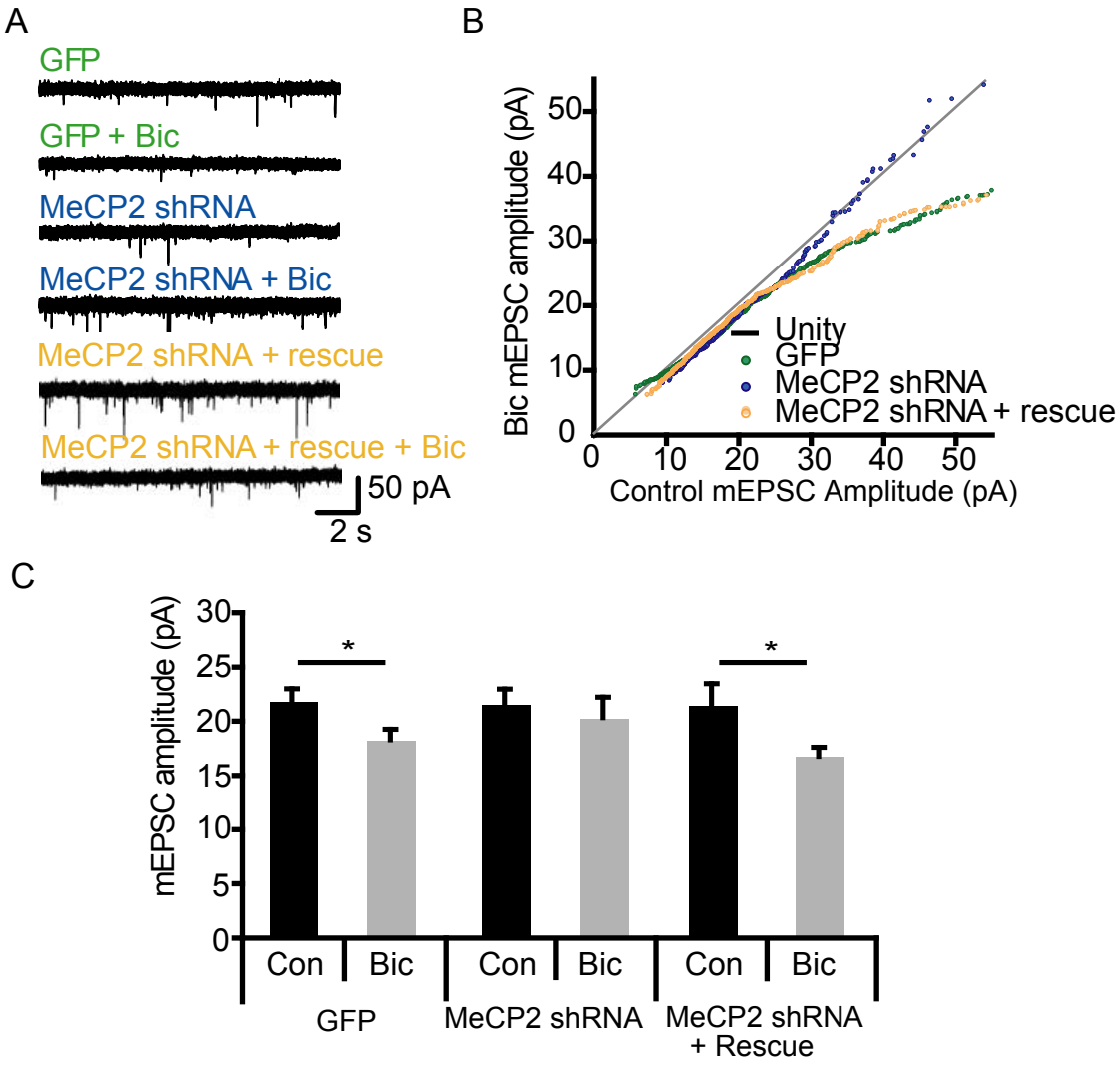

Figure 5.5 MeCP2 is required for synaptic scaling in response to elevated network activity

A. Representative 15 sec mEPSC recordings from hippocampal neurons at 14DIV, infected with GFP (control), MeCP2-shRNA, or MeCP2 shRNA plus rescue at 7 DIV. Cultures were treated with 50μM bicuculline for 48 hours prior to recording, where indicated.

B. Distributions of mEPSCs from neurons infected with GFP alone, MeCP2 shRNA, or MeCP2 shRNA + WT rescue, grown under control conditions, or treated with bicuculline for 48 hr prior to recordings. For each infection condition, control mEPSCs (x-axis) are sorted by amplitude and plotted against sorted bicuculline mEPSCs (y-axis). For clarity, only mEPSCs under 50pA are shown. The GFP control is the same data as shown in Figure 4.1 and is shown here for ease of comparison.

C. Quantification of average mEPSC amplitude (mean ± SEM) under conditions as in B. asterisk signifies $p<.05$ by t-test.

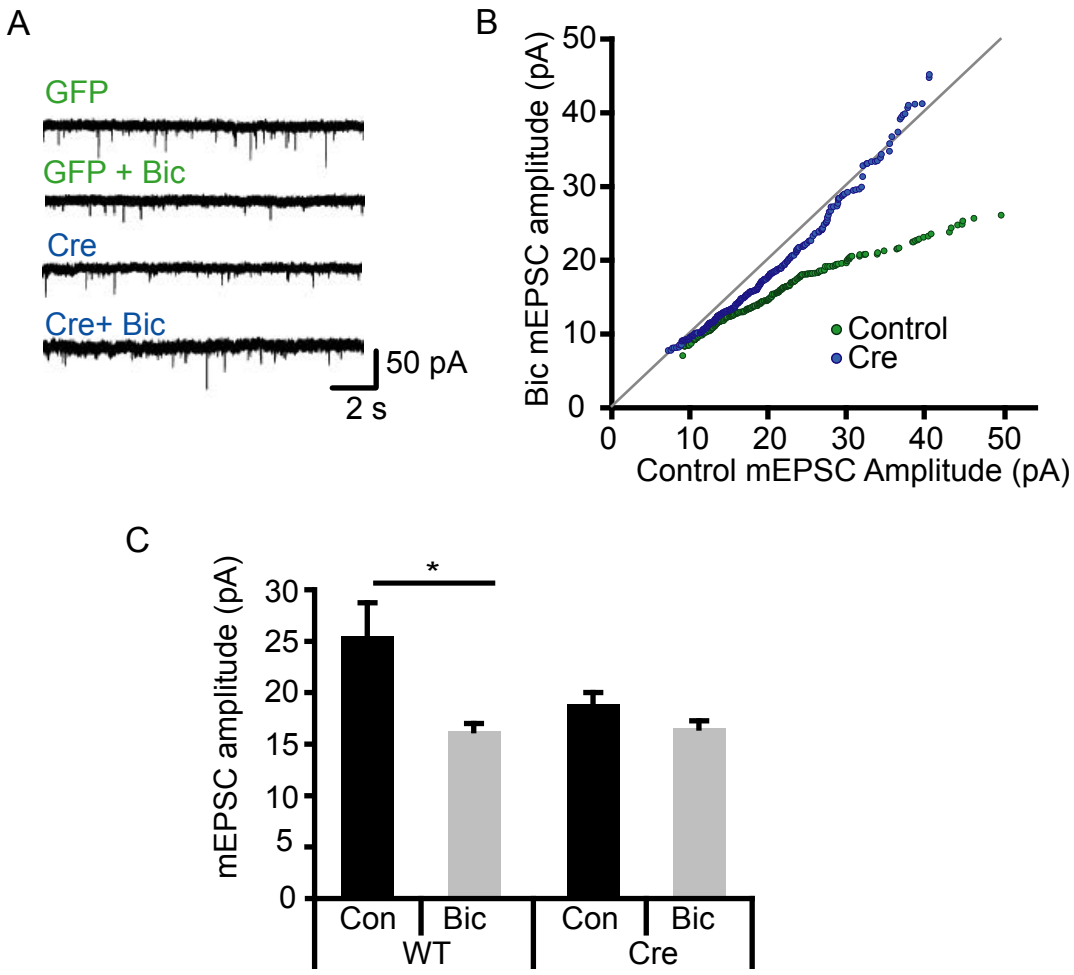

Figure 5.6 *Mecp2* null neuons do not demonstrate bicuculline induced scaling

A. Representative 15 sec mEPSC recordings from 14DIV hippocampal neurons from floxed *Mecp2* mice electroporated with GFP (control) or Cre. Cultures were treated with 50μM bicuculline for 48 hours prior to recording, where indicated.

B. Distributions of mEPSCs from floxed mecp2 neurons electroporated with GFP alone or GFP + Cre, grown under control conditions, or treated with bicuculline for 48 hr prior to recordings. For each transfection condition, control mEPSCs (x-axis) are sorted by amplitude and plotted against sorted bicuculline mEPSCs (y-axis). For clarity, only mEPSCs under 50pA are shown.

C. Quantification of average mEPSC amplitude (mean ± SEM) under conditions indicated. n= 8,5,6,7 cells. $p < 0.05$, t-test.

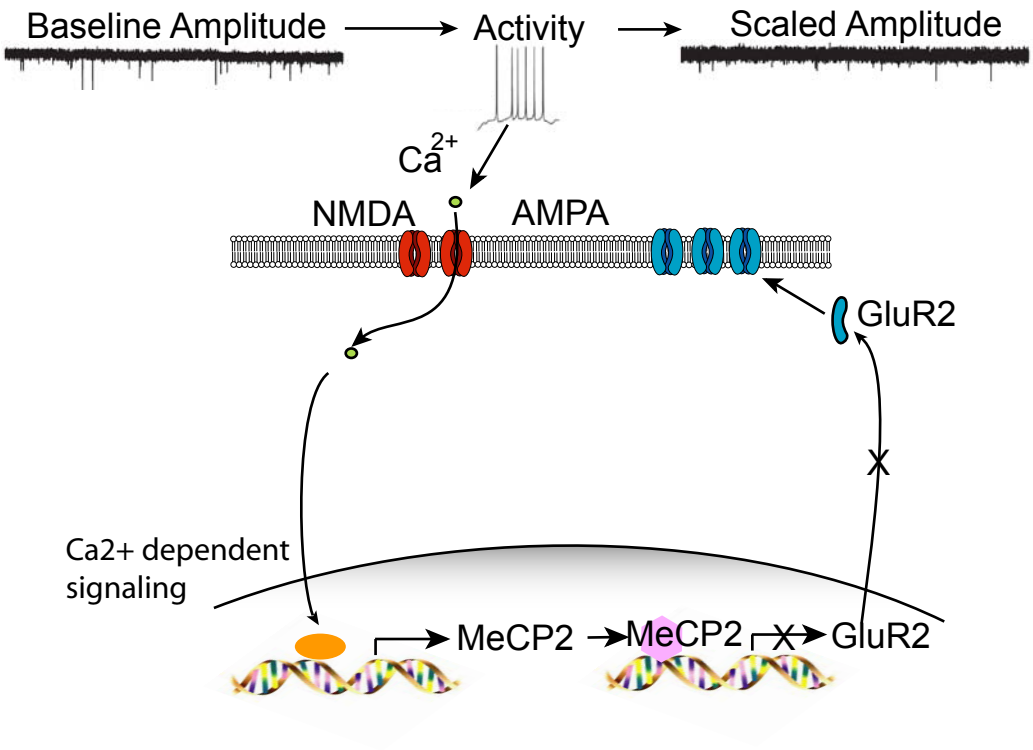

Figure 5.7 The role of MeCP2 in synaptic scaling

Bicuculline increases activity, and increased calcium influx through NMDA receptors. Elevated calcium results in an increase in MeCP2 levels. MeCP2 binds to the GluR2 promoter to repress transcription. The reduction in GluR2 protein, inconcert with increase in degradation of GluR2, reduces synaptic strength.

CHAPTER 6: DISCUSSION OF THE ROLE OF MECP2 IN HOMEOSTATIC PLASTICITY

6.1 ACTIVITY-DEPENDENT CHANGE IN NEURAL CIRCUITS

The CA1 microcircuit clearly demonstrates that the short-term dynamics of synapses are essential for network function, but synapses must also adapt to long-term changes in activity. Hebbian rules of plasticity dictate that effective synapses are strengthened and ineffective ones are eliminated. However, to maintain synaptic strength in a range suitable for information processing, the counteracting force of homeostatic plasticity scales synaptic weights in response to cell-wide changes in firing rate. Here we investigate the molecular mechanisms by which chronic activity can induce cell-wide changes in synaptic strength. We find that increases in activity increases levels of the transcriptional repressor MeCP2 and reduces expression of the AMPAR subunit GluR2. Furthermore, we show that MeCP2 binds to the GluR2 promoter. Lastly, loss of MeCP2 blocks the activity-dependent scaling down of synaptic currents. We conclude that MeCP2 is an activity-regulated gene that controls the transcription of GluR2, and that MeCP2 is necessary for activity-dependent scaling of synaptic currents (Figure 5.7).

The role of MeCP2 in synaptic scaling adds to recent evidence implicating MeCP2 in regulating various aspects of synaptic connectivity and function. While several studies have examined the role of MeCP2 in basal synaptic transmission (Dani et al., 2005; Chao et al., 2007), this is the first study that implicates MeCP2 in activity-dependent scaling of synaptic currents. The fact that MeCP2 regulates GluR2 expression is important since virtually all AMPA receptor complexes in the brain include the GluR2 subunit (Lu et al., 2009) and regulation of GluR2 expression has a direct effect on synaptic AMPA receptor subunit composition (Shi et al., 2001). We also find that increased activity leads to up-regulation of MeCP2 levels and increased occupancy

of the GluR2 promoter. Although we do not observe activity- or MeCP2-dependent regulation of GluR1 expression, it is likely that activity-dependent synaptic scaling involves changes in levels of both synaptic GluR2 and GluR1. It will be of interest to investigate the post-transcriptional mechanisms that control activity-dependent regulation of synaptic GluR1 levels.

While this study focuses on regulation of AMPA receptors by MeCP2, it is likely that this mechanism works in concert with other mechanisms that mediate activity-dependent changes in synaptic strength. Importantly, a previous study examining transcriptional control of synaptic scaling in response to elevated activity found that activity-dependent induction of polo-like kinase 2 (Plk2) leads to degradation of SPAR and synaptic weakening (Seeburg et al., 2008). Also, activity regulates the expression of Arc, which has been implicated in AMPA receptor internalization (Shepherd et al., 2006). Thus increased activity might engage multiple pathways to regulate AMPA receptor expression and trafficking to regulate synaptic currents.

6.9 SYNAPTIC DYSFUNCTION AND NEURODEGENERATIVE DISEASE

The identification of MeCP2 as a key regulator of synaptic scaling is noteworthy in terms of our understanding of Rett syndrome (RTT). RTT is a childhood neurological disorder caused by mutation in the *Mecp2* gene (Amir et al., 1999; Chahrour and Zoghbi, 2007). The relationship between *Mecp2* mutation and loss of cognitive and motor function in RTT patients is not well understood, but the associated mental retardation as well as the relatively subtle neuropathology has focused attention on the potential role of MeCP2 in the development of functional neural circuits. Regulating synaptic strength during the process of circuit formation may be particularly important to prevent uncontrolled recurrent excitation. Based on our observations we suggest that MeCP2

may play a key role in this process by mediating activity-dependent regulation of synaptic strength. Loss of this pathway due to mutations in MeCP2 may lead to a pathophysiological increase in neuronal excitability, resulting in aberrant network activity and seizures, which are common in RTT patients.

REFERENCES

Allen Mouse Brain Atlas [Internet]. Seattle (WA): Allen Institute for Brain Science. ©2009. Available from: http://mouse.brain-map.org.

Ali AB, Thomson AM (1998) Facilitating pyramid to horizontal oriens—alveus interneurone inputs: dual intracellular recordings in slices of rat hippocampus.1-16.

Ali AB, Deuchars J, Pawelzik H, Thomson AM (1998) CA1 pyramidal to basket and bistratified cell EPSPs: dual intracellular recordings in rat hippocampal slices. J Physiol 507 (Pt 1):201-217.

Amir RE, Van den Veyver IB, Wan M, Tran CQ, Francke U, Zoghbi HY (1999) Rett syndrome is caused by mutations in X-linked MECP2, encoding methyl-CpG-binding protein 2. Nat Genet 23:185-188.

Andersen P, Eccles JC, Loyning Y (1963) Recurrent inhibition in the hippocampus with identification of the inhibitory cell and its synapses. Nature 198:540-542.

Ang CW, Carlson GC, Coulter DA (2005) Hippocampal CA1 circuitry dynamically gates direct cortical inputs preferentially at theta frequencies. J Neurosci 25:9567-9580.

Ango F, di Cristo G, Higashiyama H, Bennett V, Wu P, Huang ZJ (2004) Ankyrin-based subcellular gradient of neurofascin, an immunoglobulin family protein, directs GABAergic innervation at purkinje axon initial segment. Cell 119:257-272.

Atwood HL, Karunanithi S (2002) Diversification of synaptic strength: presynaptic elements. Nat Rev Neurosci 3:497-516.

Bacci A, Coco S, Pravettoni E, Schenk U, Armano S, Frassoni C, Verderio C, De Camilli P, Matteoli M (2001) Chronic blockade of glutamate receptors enhances presynaptic release and downregulates the interaction between synaptophysin-synaptobrevin-vesicle-associated membrane protein 2. J Neurosci 21:6588-6596.

Biederer T, Scheiffele P (2007) Mixed-culture assays for analyzing neuronal synapse formation. Nature Protocols 2:670-676.

Biro AA, Holderith NB, Nusser Z (2005) Quantal size is independent of the release probability at hippocampal excitatory synapses. J Neurosci 25:223-232.

Blasco-Ibafiez JM, Freund TF (1995) Synaptic Input of Horizontal Interneurons in Stratum Oriens of the Hippocampal CA1 Subfield: Structural Basis of Feed-back Activation. European Journal of Neuroscience 7:2170-2180.

Bliss TV, Lomo T (1973) Long-lasting potentiation of synaptic transmission in the dentate area of the anaesthetized rabbit following stimulation of the perforant path. J Physiol 232:331-356.

Buzsaki G (1989) Two-stage model of memory trace formation: a role for "noisy" brain states. Neuroscience 31:551-570.

Chahrour M, Zoghbi HY (2007) The story of Rett syndrome: from clinic to neurobiology. Neuron 56:422-437.

Chao HT, Zoghbi HY, Rosenmund C (2007) MeCP2 controls excitatory synaptic strength by regulating glutamatergic synapse number. Neuron 56:58-65.

Chen RZ, Akbarian S, Tudor M, Jaenisch R (2001) Deficiency of methyl-CpG binding protein-2 in CNS neurons results in a Rett-like phenotype in mice. Nat Genet 27:327-331.

Chih B, Engelman H, Scheiffele P (2005) Control of Excitatory and Inhibitory Synapse Formation by Neuroligins. Science 307:1324-1328.

Collingridge GL, Peineau S, Howland JG, Wang YT (2010) Long-term depression in the CNS. Nat Rev Neurosci 11:459-473.

Contractor A (2002) Trans-Synaptic Eph Receptor-Ephrin Signaling in Hippocampal Mossy Fiber LTP. Science 296:1864-1869.

Croce A, Pelletier JG, Tartas M, Lacaille J-C (2010) Afferent-specific properties of interneuron synapses underlie selective long-term regulation of feedback inhibitory circuits in CA1 hippocampus. J Physiol (Lond) 588:2091-2107.

Dani VS, Chang Q, Maffei A, Turrigiano GG, Jaenisch R, Nelson SB (2005) Reduced cortical activity due to a shift in the balance between excitation and inhibition in a mouse model of Rett syndrome. Proc Natl Acad Sci U S A 102:12560-12565.

Davis GW (2006) Homeostatic control of neural activity: from phenomenology to molecular design. Annu Rev Neurosci 29:307-323.

de Wit J, Hong W, Luo L, Ghosh A (2010) Role of Leucine-Rich Repeat Proteins in the Development and Function of Neural Circuits. Annu Rev Cell Dev Biol.

de Wit J, Sylwestrak E, O'Sullivan ML, Otto S, Tiglio K, Savas JN, Iii JRY, Comoletti D, Taylor P, Ghosh A (2009a) LRRTM2 Interacts with Neurexin1 and Regulates Excitatory Synapse Formation. Neuron 64:799-806.

de Wit J, Sylwestrak E, O'sullivan ML, Otto S, Tiglio K, Savas JN, Yates III JR, Comoletti D, Taylor P, Ghosh A (2009b) LRRTM2 Interacts with Neurexin1 and Regulates Excitatory Synapse Formation. Neuron 64:799-806.

Dolan J, Walshe K, Alsbury S, Hokamp K, O'keeffe S, Okafuji T, Miller SF, Tear G, Mitchell KJ (2007) The extracellular Leucine-Rich Repeat superfamily; a comparative survey and analysis of evolutionary relationships and expression patterns. BMC Genomics 8:320.

Esumi S, Kakazu N, Taguchi Y, Hirayama T, Sasaki A, Hirabayashi T, Koide T, Kitsukawa T, Hamada S, Yagi T (2005) Monoallelic yet combinatorial expression of variable exons of the protocadherin-alpha gene cluster in single neurons. Nat Genet 37:171-176.

Fisher TE, Bourque CW (2001) The function of Ca(2+) channel subtypes in exocytotic secretion: new perspectives from synaptic and non-synaptic release. Prog Biophys Mol Biol 77:269-303.

Futai K, Kim MJ, Hashikawa T, Scheiffele P, Sheng M, Hayashi Y (2007) Retrograde modulation of presynaptic release probability through signaling mediated by PSD-95-neuroligin. Nature Neuroscience 10:186-195.

Gainey MA, Hurvitz-Wolff JR, Lambo ME, Turrigiano GG (2009) Synaptic scaling requires the GluR2 subunit of the AMPA receptor. J Neurosci 29:6479-6489.

Goold CP, Nicoll RA (2011) Single-cell optogenetic excitation drives homeostatic synaptic depression. Neuron 68:512-528.

Grooms SY, Noh KM, Regis R, Bassell GJ, Bryan MK, Carroll RC, Zukin RS (2006) Activity bidirectionally regulates AMPA receptor mRNA abundance in dendrites of hippocampal neurons. J Neurosci 26:8339-8351.

Guy J, Hendrich B, Holmes M, Martin JE, Bird A (2001) A mouse Mecp2-null mutation causes neurological symptoms that mimic Rett syndrome. Nat Genet 27:322-326.

Han K, Kim E (2008) Synaptic adhesion molecules and PSD-95. Prog Neurobiol 84:263-283.

Han Z, Buhl EH, Lorinczi S, Somogyi P (1993) High Degree of Spatial Selectivity in the Axonal and Dendritic Domains of Physiologically Identified Local-circuit Neurons in the Dentate Gyrus of the Rat Hippocampus. European Journal of Neuroscience 5:395-410.

Hattori D, Demir E, Kim HW, Viragh E, Zipursky SL, Dickson BJ (2007) Dscam diversity is essential for neuronal wiring and self-recognition. Nature 449:223-227.

Hubel DH, Wiesel TN, LeVay S (1977) Plasticity of ocular dominance columns in monkey striate cortex. Philos Trans R Soc Lond B Biol Sci 278:377-409.

Ibata K, Sun Q, Turrigiano GG (2008) Rapid synaptic scaling induced by changes in postsynaptic firing. Neuron 57:819-826.

Ju W, Morishita W, Tsui J, Gaietta G, Deerinck TJ, Adams SR, Garner CC, Tsien RY, Ellisman MH, Malenka RC (2004) Activity-dependent regulation of dendritic synthesis and trafficking of AMPA receptors. Nat Neurosci 7:244-253.

Jungling K (2006) N-Cadherin Transsynaptically Regulates Short-Term Plasticity at Glutamatergic Synapses in Embryonic Stem Cell-Derived Neurons. Journal of Neuroscience 26:6968-6978.

Kim E, Sheng M (2004) PDZ domain proteins of synapses. Nat Rev Neurosci 5:771-781.

Kim S, Burette A, Chung HS, Kwon S-K, Woo J, Lee HW, Kim K, Kim H, Weinberg RJ, Kim E (2006) NGL family PSD-95-interacting adhesion molecules regulate excitatory synapse formation. Nature Neuroscience 9:1294-1301.

Klausberger T, Magill PJ, Marton LF, Roberts JD, Cobden PM, Buzsaki G, Somogyi P (2003) Brain-state- and cell-type-specific firing of hippocampal interneurons in vivo. Nature 421:844-848.

Ko J, Kim S, Chung HS, Kim K, Han K, Kim H, Jun H, Kaang B-K, Kim E (2006) SALM synaptic cell adhesion-like molecules regulate the differentiation of excitatory synapses. Neuron 50:233-245.

Kobe B, Kajava AV (2001) The leucine-rich repeat as a protein recognition motif. Curr Opin Struct Biol 11:725-732.

Koester HJ, Johnston D (2005) Target cell-dependent normalization of transmitter release at neocortical synapses. Science 308:863-866.

Koh DS, Geiger JR, Jonas P, Sakmann B (1995) Ca(2+)-permeable AMPA and NMDA receptor channels in basket cells of rat hippocampal dentate gyrus. J Physiol 485 (Pt 2):383-402.

Krupp JJ, Vissel B, Heinemann SF, Westbrook GL (1996) Calcium-dependent inactivation of recombinant N-methyl-D-aspartate receptors is NR2 subunit specific. Mol Pharmacol 50:1680-1688.

Lacaille J-C, Mueller AL, Kunkel IDD, Schwartzkroini PA (1987) Local Circuit Interactions Between Oriens/Alveus Interneurons and CA 1 Pyramidal Cells in Hippocampal Slices: Electrophysiology and Morphology. The Journal of Neuroscience, 7:1979-1993.

Larson J, Wong D, Lynch G (1986) Patterned stimulation at the theta frequency is optimal for the induction of hippocampal long-term potentiation. Brain Res 368:347-350.

Linhoff MW, Lauren J, Cassidy RM, Dobie FA, Takahashi H, Nygaard HB, Airaksinen MS, Strittmatter SM, Craig AM (2009a) An Unbiased Expression Screen for Synaptogenic Proteins Identifies the LRRTM Protein Family as Synaptic Organizers. Neuron 61:734-749.

Lu W, Shi Y, Jackson AC, Bjorgan K, During MJ, Sprengel R, Seeburg PH, Nicoll RA (2009) Subunit composition of synaptic AMPA receptors revealed by a single-cell genetic approach. Neuron 62:254-268.

Matsuda K, Miura E, Miyazaki T, Kakegawa W, Emi K, Narumi S, Fukazawa Y, Ito-Ishida A, Kondo T, Shigemoto R, Watanabe M, Yuzaki M (2010) Cbln1 is a ligand for an orphan glutamate receptor delta2, a bidirectional synapse organizer. Science 328:363-368.

Matthews BJ, Kim ME, Flanagan JJ, Hattori D, Clemens JC, Zipursky SL, Grueber WB (2007) Dendrite self-avoidance is controlled by Dscam. Cell 129:593-604.

Mcmahon SA, Díaz E (2011) Mechanisms of excitatory synapse maturation by trans-synaptic organizing complexes. Current Opinion in Neurobiology:1-7.

Meehan RR, Lewis JD, Bird AP (1992) Characterization of MeCP2, a vertebrate DNA binding protein with affinity for methylated DNA. Nucleic Acids Res 20:5085-5092.

Momiyama A, Feldmeyer D, Cull-Candy SG (1996) Identification of a native low-conductance NMDA channel with reduced sensitivity to Mg2+ in rat central neurones. J Physiol 494 (Pt 2):479-492.

Morishita H, Yagi T (2007) Protocadherin family: diversity, structure, and function. Curr Opin Cell Biol 19:584-592.

Moulder KL, Jiang X, Taylor AA, Olney JW, Mennerick S (2006) Physiological activity depresses synaptic function through an effect on vesicle priming. J Neurosci 26:6618-6626.

Murthy VN, Schikorski T, Stevens CF, Zhu Y (2001) Inactivity produces increases in neurotransmitter release and synapse size. Neuron 32:673-682.

Myers SJ, Peters J, Huang Y, Comer MB, Barthel F, Dingledine R (1998) Transcriptional regulation of the GluR2 gene: neural-specific expression, multiple promoters, and regulatory elements. J Neurosci 18:6723-6739.

Nishimura-Akiyoshi S, Niimi K, Nakashiba T, Itohara S (2007) Axonal netrin-Gs transneuronally determine lamina-specific subdendritic segments. Proc Natl Acad Sci USA 104:14801-14806.

Nitz D, McNaughton B (2004) Differential modulation of CA1 and dentate gyrus interneurons during exploration of novel environments. J Neurophysiol 91:863-872.

O'Brien RJ, Kamboj S, Ehlers MD, Rosen KR, Fischbach GD, Huganir RL (1998) Activity-dependent modulation of synaptic AMPA receptor accumulation. Neuron 21:1067-1078.

Orban G, Kiss T, Erdi P (2006) Intrinsic and synaptic mechanisms determining the timing of neuron population activity during hippocampal theta oscillation. J Neurophysiol 96:2889-2904.

Pasterkamp RJ, Giger RJ, Ruitenberg MJ, Holtmaat AJ, De Wit J, De Winter F, Verhaagen J (1999) Expression of the gene encoding the chemorepellent semaphorin III is induced in the fibroblast component of neural scar tissue formed following injuries of adult but not neonatal CNS. Molecular and Cellular Neuroscience 13:143-166.

Plant K, Pelkey KA, Bortolotto ZA, Morita D, Terashima A, McBain CJ, Collingridge GL, Isaac JT (2006) Transient incorporation of native GluR2-lacking AMPA receptors during hippocampal long-term potentiation. Nat Neurosci 9:602-604.

Pouille F, Scanziani M (2001) Enforcement of temporal fidelity in pyramidal cells by somatic feed-forward inhibition. Science 293:1159-1163.

Pouille F, Scanziani M (2004) Routing of spike series by dynamic circuits in the hippocampus. Nature 429:717-723.

Pozo K, Goda Y (2010) Unraveling mechanisms of homeostatic synaptic plasticity. Neuron 66:337-351.

Rosenmund C, Clements JD, Westbrook GL (1993) Nonuniform probability of glutamate release at a hippocampal synapse. Science 262:754-757.

Rotstein HG, Pervouchine DD, Acker CD, Gillies MJ, White JA, Buhl EH, Whittington MA, Kopell N (2005) Slow and fast inhibition and an H-current interact to create a theta rhythm in a model of CA1 interneuron network. J Neurophysiol 94:1509-1518.

Rozov A, Burnashev N, Sakmann B, Neher E (2001) Transmitter release modulation by intracellular Ca2+ buffers in facilitating and depressing nerve terminals of pyramidal cells in layer 2/3 of the rat neocortex indicates a target cell-specific difference in presynaptic calcium dynamics. J Physiol 531:807-826.

Rutishauser U, Acheson A, Hall AK, Mann DM, Sunshine J (1988) The neural cell adhesion molecule (NCAM) as a regulator of cell-cell interactions. Science 240:53-57.

Scheiffele P (2003) Neurexin mediate the assembly of presynaptic terminals.1-9.

Scheiffele P, Fan J, Choih J, Fetter R, Serafini T (2000) Neuroligin Expressed in Nonneuronal Cells Triggers Presynaptic Development in Contacting Axons.1-13.

Seeburg DP, Feliu-Mojer M, Gaiottino J, Pak DT, Sheng M (2008) Critical role of CDK5 and Polo-like kinase 2 in homeostatic synaptic plasticity during elevated activity. Neuron 58:571-583.

Shen K, Scheiffele P (2010) Genetics and Cell Biology of Building Specific Synaptic Connectivity. Annu Rev Neurosci 33:473-507.

Shepherd JD, Rumbaugh G, Wu J, Chowdhury S, Plath N, Kuhl D, Huganir RL, Worley PF (2006) Arc/Arg3.1 mediates homeostatic synaptic scaling of AMPA receptors. Neuron 52:475-484.

Shi S, Hayashi Y, Esteban JA, Malinow R (2001) Subunit-specific rules governing AMPA receptor trafficking to synapses in hippocampal pyramidal neurons. Cell 105:331-343.

Skene PJ, Illingworth RS, Webb S, Kerr AR, James KD, Turner DJ, Andrews R, Bird AP (2010) Neuronal MeCP2 is expressed at near histone-octamer levels and globally alters the chromatin state. Mol Cell 37:457-468.

Söllner C, Wright GJ (2009) A cell surface interaction network of neural leucine-rich repeat receptors. Genome Biol 10:R99.

Song JY, Ichtchenko K, Sudhof TC, Brose N (1999) Neuroligin 1 is a postsynaptic cell-adhesion molecule of excitatory synapses. Proc Natl Acad Sci U S A 96:1100-1105.

Song MR, Ghosh A (2004) FGF2-induced chromatin remodeling regulates CNTF-mediated gene expression and astrocyte differentiation. Nat Neurosci 7:229-235.

Sun HY, Dobrunz LE (2006) Presynaptic kainate receptor activation is a novel mechanism for target cell-specific short-term facilitation at Schaffer collateral synapses. J Neurosci 26:10796-10807.

Sun HY, Lyons SA, Dobrunz LE (2005) Mechanisms of target-cell specific short-term plasticity at Schaffer collateral synapses onto interneurones versus pyramidal cells in juvenile rats. J Physiol 568:815-840.

Sutton MA, Ito HT, Cressy P, Kempf C, Woo JC, Schuman EM (2006) Miniature neurotransmission stabilizes synaptic function via tonic suppression of local dendritic protein synthesis. Cell 125:785-799.

Thiagarajan TC, Lindskog M, Tsien RW (2005) Adaptation to synaptic inactivity in hippocampal neurons. Neuron 47:725-737.

Thompson WJ (1985) Activity and synapse elimination at the neuromuscular junction. Cell Mol Neurobiol 5:167-182.

Turrigiano G (2007) Homeostatic signaling: the positive side of negative feedback. Curr Opin Neurobiol 17:318-324.

Turrigiano GG (2008) The self-tuning neuron: synaptic scaling of excitatory synapses. Cell 135:422-435.

Turrigiano GG, Leslie KR, Desai NS, Rutherford LC, Nelson SB (1998) Activity-dependent scaling of quantal amplitude in neocortical neurons. Nature 391:892-896.

Tzingounis AV, Nicoll RA (2006) Arc/Arg3.1: linking gene expression to synaptic plasticity and memory. Neuron 52:403-407.

Uemura T, Lee SJ, Yasumura M, Takeuchi T, Yoshida T, Ra M, Taguchi R, Sakimura K, Mishina M Trans-synaptic interaction of GluRdelta2 and Neurexin through Cbln1 mediates synapse formation in the cerebellum. Cell 141:1068-1079.

Uemura T, Lee S-J, Yasumura M, Takeuchi T, Yoshida T, Ra M, Taguchi R, Sakimura K, Mishina M (2010) Trans-Synaptic Interaction of GluRδ2 and Neurexin through Cbln1 Mediates Synapse Formation in the Cerebellum. Cell 141:1068-1079.

Ullrich B, Ushkaryov YA, Sudhof TC (1995) Cartography of neurexins: more than 1000 isoforms generated by alternative splicing and expressed in distinct subsets of neurons. Neuron 14:497-507.

Vanderwolf CH (1969) Hippocampal electrical activity and voluntary movement in the rat. Electroencephalogr Clin Neurophysiol 26:407-418.

Varoqueaux F, Aramuni G, Rawson RL, Mohrmann R, Missler M, Gottmann K, Zhang W, Sudhof TC, Brose N (2006) Neuroligins determine synapse maturation and function. Neuron 51:741-754.

Vicini S, Wang JF, Li JH, Zhu WJ, Wang YH, Luo JH, Wolfe BB, Grayson DR (1998) Functional and pharmacological differences between recombinant N-methyl-D-aspartate receptors. J Neurophysiol 79:555-566.

Wang Y (2004) Anatomical, physiological and molecular properties of Martinotti cells in the somatosensory cortex of the juvenile rat. J Physiol (Lond) 561:65-90.

Wierenga CJ, Ibata K, Turrigiano GG (2005) Postsynaptic expression of homeostatic plasticity at neocortical synapses. J Neurosci 25:2895-2905.

Williams ME, Wilke SA, Daggett A, Davis E, Otto S, Ravi D, Ripley B, Bushong EA, Ellisman MH, Klein G, Ghosh A Cadherin-9 regulates synapse-specific differentiation in the developing hippocampus. Neuron 71:640-655.

Woo J, Kwon S-K, Kim E (2009) The NGL family of leucine-rich repeat-containing synaptic adhesion molecules. Molecular and Cellular Neuroscience:1-10.

Wu LG, Saggau P (1994) Presynaptic calcium is increased during normal synaptic transmission and paired-pulse facilitation, but not in long-term potentiation in area CA1 of hippocampus. J Neurosci 14:645-654.

Zhou Z, Hong EJ, Cohen S, Zhao WN, Ho HY, Schmidt L, Chen WG, Lin Y, Savner E, Griffith EC, Hu L, Steen JA, Weitz CJ, Greenberg ME (2006) Brain-specific phosphorylation of MeCP2 regulates activity-dependent Bdnf transcription, dendritic growth, and spine maturation. Neuron 52:255-269.

Zhu JJ, Esteban JA, Hayashi Y, Malinow R (2000) Postnatal synaptic potentiation: delivery of GluR4-containing AMPA receptors by spontaneous activity. Nat Neurosci 3:1098-1106.

Zhu JJ, Qin Y, Zhao M, Van Aelst L, Malinow R (2002) Ras and Rap control AMPA receptor trafficking during synaptic plasticity. Cell 110:443-455.

Zucker RS, Regehr WG (2002) Short-term synaptic plasticity. Annu Rev Physiol 64:355-405.